HELSINKI INSTITUTE OF PHYSICS   INTERNAL REPORT SERIES

Primordial Perturbations from a Self-interacting Curvaton

Olli Taanila

Helsinki Institute of Physics
University of Helsinki
Finland

ACADEMIC DISSERTATION

*To be presented, with the permission of the Faculty of Science
of the University of Helsinki, for public criticism
in the auditorium CK112 of Exactum, Gustaf Hällströmin katu 2 B,
on the 15th of December 2010 at 10 o'clock.*

Helsinki 2010

Acknowledgements

I have the privilege to thank my supervisor Kari Enqvist. For the past few years that I have been working with him, we have shared many interesting and entertaining discussions. He has not only been an excellent supervisor, but I also consider him to be a relaxed yet enthusiastic colleague. Moreover, we apparently share a similar view on how to serve green asparagus. Another significant mentor of mine has been Keijo Kajantie, who was the person originally responsible for hiring me to the department. As a friend of ours once said, Keijo has a very admirable attitude towards both science and life.

Gerasimos Rigopoulos, Anders Tranberg and Patta Yogendran have tutored me in my early steps of research, and for that I am very grateful. They have taught me a lot about physics, especially the more practical side of it. I also wish to thank Anders Tranberg for reading the manuscript and offering many insightful comments on it. Similarly I wish to thank the referees of the thesis, Arttu Rajantie and Shinta Kasuya, for valuable comments.

I also wish to thank my other collaborators, namely Anupam Mazumdar, Sami Nurmi, Philip Stephens and Tomo Takahashi. They have all made our collaboration fun and eased, yet insightful and fruitful. It has been an enjoyable experience to work on these papers with all of them.

During my undergraduate and graduate studies in Helsinki I have been priviledged to attend many excellent courses. Of the exceptional teachers in the department one must mention Claus Montonen, Hannu Kurki-Suonio and especially Juha Honkonen. There have also been an enormous number of officemates and co-students with whom I have had the pleasure not only to study, but to also babble about all things between end of inflation and our exercises, and I want to thank them all. Especially I want to acknowledge the trio of noisiest theoretical physics graduate students Helsinki has ever known, with whom I have enjoyed countless hours of badminton.

Last but not least I wish to thank my parents and my significant other for support and not-too-loud criticism of my choice of career.

Helsinki, November 2010

Olli Taanila

Abstract

Inflation is a period of accelerated expansion in the very early universe, which has the appealing aspect that it can create primordial perturbations via quantum fluctuations. These primordial perturbations have been observed in the cosmic microwave background, and these perturbations also function as the seeds of all large-scale structure in the universe. Curvaton models are simple modifications of the standard inflationary paradigm, where inflation is driven by the energy density of the inflaton, but another field, the curvaton, is responsible for producing the primordial perturbations.

Since the curvaton must decay, it must have some interactions. Additionally realistic curvaton models typically have some self-interactions. In this work we consider self-interacting curvaton models, where the self-interaction is a monomial in the potential, suppressed by the Planck scale, and thus the self-interaction is very weak. Nevertheless, since the self-interaction makes the equations of motion non-linear, it can modify the behaviour of the model very drastically. The most intriguing aspect of this behaviour is that the final properties of the perturbations become highly dependent on the initial values.

Departures of Gaussian distribution are important observables of the primordial perturbations. Due to the non-linearity of the self-interacting curvaton model and its sensitivity to initial conditions, it can produce significant non-Gaussianity of the primordial perturbations. In this work we investigate the non-Gaussianity produced by the self-interacting curvaton, and demonstrate that the non-Gaussianity parameters do not obey the analytically derived approximate relations often cited in the literature.

Furthermore we also consider a self-interacting curvaton with a mass in the TeV-scale. Motivated by realistic particle physics models such as the Minimally Supersymmetric Standard Model, we demonstrate that a curvaton model within the mass range can be responsible for the observed perturbations if it can decay late enough.

List of Publications

The content of this thesis is based on the following research articles [1–3]:

I   **The Subdominant Curvaton**,
K. Enqvist, S. Nurmi, G. Rigopoulos, O. Taanila and T. Takahashi,
JCAP **0911** (2009) 003.

II   **Non-Gaussian Fingerprints of Self-Interacting Curvaton**,
K. Enqvist, S. Nurmi, O. Taanila and T. Takahashi,
JCAP **1004** (2010) 009.

III **The TeV-mass Curvaton**,
K. Enqvist, A. Mazumdar and O. Taanila,
JCAP **1009** (2010) 030.

In all of the papers the authors are listed alphabetically according to the particle physics convention.

The Author's Contribution to the Joint Publications

I   The inital idea to study subdominant curvaton models was T. Takahashi's. The present author performed the initial analytical calculations and wrote a computer program to solve the model numerically. Excluding the analytical treatise which was written by S. Nurmi, and the section concerning the Fokker-Planck equation which was written by G. Rigopoulos, the present author wrote the first draft of the paper, which was then polished jointly by all authors.

II   The program developed for **I** was further improved by the present author by implementing a method to calculate the non-Gaussianity parameters. The present author calculated all the results and produced all of the plots, as well as wrote the first draft of the paper.

III The pre-existing code was used by the present author to calculate the results. Also the analytical calculations were mostly done by the present author. A. Mazumdar wrote the parts of the draft discussing MSSM and Q-balls and K. Enqvist the introduction and discussion. The rest was drafted by the present author and then polished jointly with K. Enqvist.

Units and Conventions

In this work we use natural units, i.e., we set three constants of nature to unity,

$$\hbar = c = k_{\mathrm{B}} = 1 \ .$$

For most of this work, we use units of electronvolts, eV, or multiples thereof, such as gigaelectronvolts, GeV, as the measure of energy and consequently all dimensionful quantities.

We denote the reduced Planck mass by

$$M_{\mathrm{Pl}} = \sqrt{\frac{\hbar c}{8\pi G}} \ .$$

In the three papers, on which this thesis is based, we set the reduced Planck mass often to unity, i.e., express all dimensionful variables as powers of M_{Pl}. Nevertheless, we refrain from setting it to unity in the main text.

For Fourier transforms we use the normalization convention where the factors of 2π are included in the inverse transformation,

$$f(\mathbf{x}) = \int \frac{\mathrm{d}^3\mathbf{k}}{(2\pi)^3} e^{i\mathbf{k}\cdot\mathbf{x}} f_{\mathbf{k}} \quad , \qquad f_{\mathbf{k}} = \int \mathrm{d}^3\mathbf{x}\, e^{-i\mathbf{k}\cdot\mathbf{x}} f(\mathbf{x}) \ .$$

As most of this work is concerned with investigating the evolution of certain quantities from the end of inflation to some much later point in time, we adopt the short-hand notation where the subscript $*$ denotes a quantity evaluated at the end of inflation, e.g. H_* is the Hubble constant at the end of inflation.

In the literature there has been a mixture of notations concerning the factor r. It denotes the energy density of the curvaton ρ_σ compared with the total energy density of the universe. For this work we adopt a very useful, though a bit inconsistent notation where r denotes the energy fraction in the curvaton field,

$$r \equiv \frac{\rho_\sigma}{\Sigma_i \rho_i} \ ,$$

while r_* describes the energy density of the curvaton compared to that of the background at the end of inflation,

$$r_* \equiv \left. \frac{\rho_\sigma}{\rho_{\mathrm{r}}} \right|_{\text{end of inflation}} \ ,$$

and r_{dec}, in discrepancy with the preceding definition of r, measures the quantity often referred to as r in the literature,

$$r_{\text{dec}} \equiv \left. \frac{3\rho_\sigma}{3\rho_\sigma + 4\rho_{\text{r}}} \right|_{\text{curvaton decay}},$$

also called the efficiency factor. Note that these definitions somewhat differ from the notation used in the attached publications.

Contents

Chapter 1

Introduction

Modern cosmology offers a detailed description of the evolution of the universe from its very first picoseconds until the present day. It predicts accurately the amount of different elements present in the universe [4–6], and it explains the evolution of structure on large scales as well as the formation of non-linear structures on smaller scales. This standard description of the universe is often called Λ_{CDM}, comparable to the Standard Model of particle physics. Λ_{CDM} however has several ingredients which invite a more rigorous understanding: What is the nature of dark matter and dark energy, what is the source of the baryon asymmetry in the universe, and what is the mechanism for inflation in the very early universe?

The topic of this thesis is the generation of primordial perturbations in *curvaton models*. The primordial perturbations are usually thought to originate during inflation, and they function as the primordial seeds for all structure in the universe: stars, galaxies, clusters etc. The curvaton models are a modification of the run-of-the-mill inflationary models.

1.1   Friedmann-Robertson-Walker Cosmology

The universe is described exceptionally well by a spatially homogeneous and isotropic universe. The most generic metric realizing these symmetries is the *Friedmann-Robertson-Walker* cosmology [7–11], described by the metric

$$ \mathrm{d}s^2 = -\mathrm{d}t^2 + a^2(t)\left(\frac{\mathrm{d}r^2}{1 - Kr^2} + r^2\mathrm{d}\theta^2 + r^2\sin^2\theta\,\mathrm{d}\theta^2\right). \qquad (1.1) $$

Here K determines the geometry of slices of constant time: The case $K = -1$ corresponds to a hyperbolic universe, $K = 1$ corresponds to a closed universe, and $K = 0$ to a flat universe. Observationally we know that K is extremely close to zero [12, 13], and thus henceforth we set it to zero.

The scale factor $a(t)$ encodes information about the evolution of distances in the universe, and its evolution determines the expansion of the universe. Due to the aforementioned symmetries of the FRW-model, the scale factor can have evolution only in time. The time evolution of $a(t)$ is determined by the energy content of the universe. The equation of motion for $a(t)$ is to be derived from equations of motion for the whole metric, which in general relativity are given by the Einstein equations

$$R_{\mu\nu} - \frac{1}{2} R g_{\mu\nu} = 8\pi G T_{\mu\nu} \,. \tag{1.2}$$

Here the metric $g_{\mu\nu}$ is the fundamental dynamical quantity, whereas R and $R_{\mu\nu}$ are respectively the Ricci scalar and the Ricci tensor, which encode information of the curvature of the metric. They consist of derivatives of $g_{\mu\nu}$, and their computation is discussed in more detail in section 2.3.

The information about the energy content of the universe is given by the energy momentum tensor. In the rest frame of an ideal fluid the energy-momentum tensor can be written as $T^\nu_\mu = \mathrm{diag}(-\rho, p, p, p)$, and thus the continuity equation $\nabla_\mu T^{\mu\nu} = 0$, analogous to the energy and momentum conservation in flat space, can be written as

$$\dot{\rho} + 3H(\rho + p) = 0 \,,$$

where ρ and p are the energy density and pressure, and H is the Hubble parameter, $H \equiv \dot{a}/a$, which measures the expansion speed of the universe. For a fluid with a constant equation of state parameter $w \equiv p/\rho$, a scaling law can thus be written (see also section 3.2 for the case of homogeneous oscillating fields) for the energy density:

$$\rho(t) \propto a^{-3(1+w)}(t) \,.$$

The Einstein equation (1.2) has two free indices, and is thus actually a set of $4 \times 4 - 6 = 10$ equations. Nevertheless, due to the symmeries of the FRW metric only very few of the equations are independent. Writing the $0 - 0$ and $i - i$ components separately, and substracting them from each other, one ends up with the Friedmann equations,

$$H^2 = \left(\frac{\dot{a}}{a}\right)^2 = \frac{8\pi G}{3}\rho \tag{1.3}$$

$$\frac{\ddot{a}}{a} = -\frac{4\pi G}{3}(\rho + 3p) \,. \tag{1.4}$$

Here the dot denotes the usual temporal derivative,

$$\dot{} \equiv \frac{d}{dt} \,.$$

The Friedmann equations encode the information of how the energy content of the universe affects the expansion of the universe. The scale factor $a(t)$ in the metric of the equation (1.1) is thus to be solved for in the Friedmann equations.

The coordinates in equation (1.1) correspond to physical time and comoving spatial coordinates, meaning that while the time coordinate t is the actual time measured by a comoving observer, the fixed coordinate distances correspond to increasing physical distances due to the evolution of $a(t)$. Often it is more convenient to use *conformal time η*, defined by the infinitesimal expression

$$\mathrm{d}\eta = \frac{\mathrm{d}t}{a(t)} \ .$$ (1.5)

Intuitively this means that the new time coordinate scales according to the evolution of $a(t)$, similarly to the spatial coordinates. The metric in these new coordinates reads

$$\mathrm{d}s^2 = a^2(\eta)\Big(-\mathrm{d}\eta^2 + \mathrm{d}x^i\,\mathrm{d}x^i \Big) \ .$$

As with the physical time t, we define a temporal derivative with respect to the conformal time η,[1]

$$' \equiv \frac{d}{d\eta} \ .$$

We also define the conformal Hubble parameter,

$$\mathcal{H} \equiv \frac{a'}{a} \ .$$

Using conformal time can often simplify calculations. We alternate between using physical and conformal time from calculation to calculation according to which choice makes the notation simplest.

1.2 The Hot Big Bang and the CMB

Several observations, including the redshift of distant galaxies [14], are explained by the expansion of the universe [7]. Indeed, solving for the evolution of the scale factor $a(t)$ by inputting the energy content of the universe into the Friedmann equation results in an expanding solution. The consequence of the expansion is of course that as we go back in time the universe becomes more dense and correspondingly hotter. This is the basic idea that we call the hot Big Bang.

Some of the most concrete evidences for the hot Big Bang is the cosmic microwave background, or CMB [15]. In the very early universe the temperature of the primordial plasma was very high, and thus the plasma was completely ionized. After large amount of expansion, the temperature dropped sufficiently for the plasma to start to recombine into electrically neutral atoms. As the universe turned electrically neutral, the mean free path of photons suddenly increased by several orders of magnitude and the photons started to propagate effectively freely. While these photons had

---

[1]Note that $'$ is used to denote a derivative not only with respect to conformal time but also with respect to a scalar field. Nonetheless, it is usually clear from the context what is meant with this notation.

a large energy early on, i.e., the temperature of decoupling, the photons have been redshifted by the expansion of the universe all the way to the microwave part of the electromagnetic spectrum in current times, and thus the microwave photons produce a background: Everywhere we look in the sky we can observe the microwave radiation originating from the primordial universe. The measurement of the CMB [13, 16, 17] and the intricacies of its spectrum is the source of the most accurate and reliable information about the early universe, and thus it is referred to in this work on several occasions.

1.3   Inflation

While standard Big Bang cosmology is otherwise extremely successful in explaining the observable universe, it has trouble explaining the initial conditions which are required for the evolution of the universe to match observations.

The CMB, which encodes information about the variations in energy density in the early universe, is extremely homogeneous; in fact, it has temperature perturbations with a relative magnitude of only 10^{-5}. However, the (comoving) diameter of the sky that we observe today is much larger than the length of causal propagation from the Big Bang until CMB decoupling. This means that the different regions in the CMB sky appear to have had no causal contact with the other regions, yet they all still have the same properties, near perfect homogeneity and isotropy. How can these regions have the same temperature if they have never been in contact with each other? This is called the *the horizon problem*.

Furthermore, the spatial geometry of the universe is extremely flat. The energy density of the universe is extremely close to the critical density $\rho_c \equiv 3H^2/8\pi G$, or $\Omega \equiv \rho/\rho_c \simeq 1$. However, $\Omega = 1$ is typically not an attractor, but rather an unstable value. This can be seen by writing the evolution equation for Ω [18]

$$\frac{d\Omega}{d\ln a} = (1 + 3w)\Omega(\Omega - 1) \ , \tag{1.6}$$

where w is the equation of state parameter of the constituents of the universe. This clearly states that for $w > -\frac{1}{3}$, $\Omega = 1$ is unstable. Thus if Ω is so close to its critical value now, Ω must have been extremely close to the critical value in the very early universe. Can we explain why this was so? This problem is called *the flatness problem*.

The solution to these problems is *inflation*, as suggested by Guth in 1981 [19] with similar ideas already put forward earlier by Starobinsky [20, 21]. The idea is that the radiation driven thermal expansion history of the universe is modified by a period of exponential or quasi-exponential expansion of the universe early on. After several number of e-folds, the universe *reheats* in a process where the energy driving inflation decays into ordinary degrees of freedom, after which the standard thermal history continues.

Inflationary universe corresponds to the Friedmann-Robertson-Walker-universe with

$$a(t) \propto e^{Ht} \ .$$

This space is also called *de Sitter space*. Using the first Friedmann equation (1.3), we get

$$\rho = 3M_{\text{Pl}}^2 H^2 \ .$$

This means that since H is constant, so is the energy density. Since

$$\rho \propto a^{-3(1+w)} \ ,$$

we can also conclude that $w = -1$, fulfilling the condition of equation (1.6). This means that inflation is caused by any energy component with an energy density which does not dilute in the expansion of the universe.

In conformal coordinates, integrating equation (1.5), we get

$$a(\eta) = -\frac{1}{H\eta} \ ,$$

where now the conformal time runs from $-\infty$, corresponding to infinite past, to 0, corresponding to infinite future.

The original idea by Guth was that a scalar field would sit in a false vacuum, and that the potential energy of this false vacuum would drive inflation. However, this model was plagued with the problem of graceful exit: The false vacuum driven inflation would never end. After several generations of inflationary paradigms, *slow-roll inflation* [22–25] is nowadays considered to be the most well-accepted paradigm, and several particle physics motivated models have been presented (for a review see e.g. [26]).

Slow-roll Inflation

In single field slow-roll inflation, inflation is driven by a scalar field slowly rolling down its potential — hence the name. A homogeneous scalar field with an action

$$S = \int \mathrm{d}^4 x \sqrt{-g} \left[-\frac{1}{2} \partial_\mu \varphi \, \partial^\mu \varphi - V(\varphi) \right]$$

has the pressure and energy density given by

$$\rho = \frac{1}{2}\dot{\varphi}^2 + V(\varphi) \quad , \quad p = \frac{1}{2}\dot{\varphi}^2 - V(\varphi) \ . \tag{1.7}$$

The equation of state parameter is then given by

$$w = \frac{p}{\rho} = \frac{\frac{1}{2}\dot{\varphi}^2 + V(\varphi)}{\frac{1}{2}\dot{\varphi}^2 - V(\varphi)} \ .$$

Hence, if the potential energy of the field dominates its kinetic term, w can be close to (but not smaller than) -1, and inflation ensues. This means slow evolution of the field in the sense that $\langle \frac{1}{2}\dot{\varphi}^2 \rangle < V(\varphi)$. Slow-roll inflation then corresponds to the limit $\frac{1}{2}\dot{\varphi}^2 \ll V(\varphi)$.

Typically slow-roll inflation is parameterized by the so called slow-roll parameters. The first of them, ε, is defined by

$$\varepsilon = \frac{M_{\mathrm{Pl}}^2}{2}\left(\frac{V'}{V}\right)^2 , \tag{1.8}$$

where the prime denotes a derivative with respect to the field. ε describes the slope of the potential at the point of inflation, and has to be small enough in order for the kinetic energy to be sufficiently small. The limit $\varepsilon = 0$ corresponds here to the exact de Sitter space limit.

The other slow-roll parameter is η,[2] defined by

$$\eta = M_{\mathrm{Pl}}^2 \frac{V''}{V} . \tag{1.9}$$

η measures the curvature of the potential at the point of inflation. If ε is small, inflation ensues, however its duration is controlled by the magnitude of η: The potential has to be flat enough in order for the acceleration of the field to be small enough.

Quite soon after the idea of inflation was presented, it was also realised in [27–29] based on the work of [30], that inflation offers a natural mechanism to produce the density perturbations of the universe. This property of inflation is nowadays considered to be perhaps the most convincing argument for inflation, and it is also the main topic of this thesis.

1.4   Primordial Perturbations

The cosmic microwave background, which offers us our best view into the primordial universe, has been observed to be extremely homogeneous [31, 32]. In fact, aside from the dipole of the CMB which is due to the peculiar motion of our galaxy and the solar system, the relative temperature perturbations in the CMB have the relative amplitude of $\sim 10^{-5}$. It is however these small perturbations that we are interested in.

Observations on the later universe [33, 34] confirm that on large scale (i.e., on scales much larger than clusters) the universe is very homogeneous. Nevertheless, the smaller scales are populated by rich structure, e.g. galaxies, clusters, superclusters, and quite importantly, stars and planets. These structures are formed by gravitational collapse in what is called hierarchical structure formation: Structure starts to form

---

[2]η is also used to denote conformal time, as is ε other quantities. Since ε and η are mainly used in this section, we however use the traditional notation here.

by gravitational collapse first on the smallest scales, and later on in the larger scales. An important ingredient in hierarchical structure formation are the same primordial perturbations that we observe in the CMB: These perturbations act as the initial seed for structure. Small initial overdensities will collapse to form first protostars, and later on galaxies and clusters.

To quantify the initial perturbations, we use several observables. The most important of them is the amplitude of the perturbations, which is often expressed by the power spectrum (defined later in equation (2.19)). The amplitude for the power spectrum at astrophysical scales is given by

$$\frac{2}{5}\sqrt{\mathcal{P}_{\mathcal{R}}} = 1.91 \times 10^{-5} \, , \tag{1.10}$$

often called the COBE normalization according to the first experiment to measure the perturbations accurately. Another observable is the spectral index, which expresses how blue- or red-tilted the spectrum is, i.e., whether there are more over and underdensities in the smaller or larger scales. Observations are consistent with the spectral index being unity, meaning that the perturbations have been observed to be almost scale-invariant. Yet another observational quantity is the amount of non-Gaussianity in the primordial perturbations. This is usually quantified by the non-Gaussianity parameters f_{NL} and g_{NL} as discussed in chapter 4. The current observational limits are consistent with f_{NL} and g_{NL} being zero. Thus we can conclude that the primordial perturbations have been observed to be nearly scale-invariant, extremely Gaussian, and they have the relative amplitude of $\sim 10^{-5}$.

One of the biggest triumphs of the inflationary paradigm is that it offers a natural mechanism to produce these initial perturbations, as is explained in chapter 3. In the inflating universe the quantum fluctuations of fields are expanded to very large scales and they turn into classical perturbations. Indeed, the properties of the primordial perturbations offer us most of the little (indirect) observational insight into inflation that we have. If not taking into account the properties of the primordial perturbations, we know actually very little of inflation, mainly that it happened in relatively high energy scale and lasted long enough for the scale factor to grow at least by a factor of e^{60}.

Chapter 2

Cosmological Perturbation Theory

To study the formation and evolution of density perturbations in the universe, we need to develop cosmological perturbation theory. This means adding small perturbations to the FRW universe, and seeing how these perturbations evolve. We consider here only linear theory, and ignore all possible backreaction of the perturbations on the background solution.

2.1   The Perturbed Metric and Gauge Transformations

Adding perturbations to the metric of the background solution, we get

$$g_{\mu\nu} = a^2(\eta_{\mu\nu} + h_{\mu\nu}) ,$$

where $\eta_{\mu\nu}$ is the flat metric of Minkowski space. The perturbations can now be written[1]

$$[h_{\mu\nu}] = \left[\begin{array}{cc} -2A & -B_i \\ -B_i & -2D\delta_{ij} + 2E_{ij} \end{array} \right] ,$$

or expressing this in terms of the line element,

$$\mathrm{d}s^2 = a^2(\eta)\left\{ -(1+2A)\mathrm{d}\eta^2 - 2B_i\,\mathrm{d}\eta\,\mathrm{d}x^i + \left[(1+2D)\delta_{ij} + 2E_{ij}\right]\mathrm{d}x^i\mathrm{d}x^j \right\} . \quad (2.1)$$

Here we work in conformal time, since it simplifies the notation a bit for the time being.

---

[1] The components of a tensor are, of course, not tensors. Thus, even though the notation $A(\eta, x)$, $E_{ij}(\eta, x)$ etc. is similar to real tensors, bear in mind that the scalar perturbations are *not* tensors.

Naïvely the above metric has $1 + 3 + 1 + 5 = 10$ degrees of freedom. A general gauge transformation has 4 degrees of freedom, corresponding to a 4-vector, and thus, the metric has 6 *physical* degrees of freedom. The physical degrees of freedom can be furthermore divided into scalar, vectorial and tensorial degrees of freedom. By dividing the tensorial part into a trace, a traceless tensor, and a gradient of a vector, and then the vector fields to two parts, the first one with zero curl and the second one with zero divergence, we can write

$$
[h_{\mu\nu}] = \begin{bmatrix} -2A & B_{,i} - B_i^V \\ B_{,i} - B_i^V & 2D + E_{,ij} - \frac{1}{3}\delta_{ij}\delta^{kl}E_{,kl} - \frac{1}{2}(E_{i,j} + E_{j,i}) + E_{ij}^T \end{bmatrix} .
\tag{2.2}
$$

Here now E_{ij}^T is transverse and traceless, and B_i^V has zero divergence.

According to the decomposition theorem (see e.g. [35, 36]), perhaps quite suprisingly, the scalar, vectorial and tensorial degrees of freedom do not interact in first order perturbation theory. Indeed, vector perturbations have only decaying solutions, where as the tensorial modes obey a wave equation, and are responsible for gravity waves. We are interested in the perturbations in the density of matter (i.e., the temperature of the CMB) or alternatively the curvature of space. These correspond to scalar modes, and thus, because of the decomposition theorem, to follow their evolution we can solve for them without caring what happens to the other DOFs. However, it is noteworthy that since the decomposition theorem applies only at first order in perturbation theory, second order vector and tensor perturbations are generated automatically even if they were initially zero [37].

With only the scalar perturbations the metric reads

$$
ds^2 = a^2(\eta)\left\{-(1+2A)d\eta^2 + 2B_{,i}\,d\eta\,dx^i + \left[(1-2\psi)\delta_{ij} + 2E_{,ij}\right]dx^i\,dx^j\right\},
\tag{2.3}
$$

where we have defined

$$
\psi \equiv D + \frac{1}{3}\nabla^2 E .
$$

A general (infinitesimal) coordinate transformation has four degrees of freedom,

$$
\tilde{x}^\alpha = x^\alpha + \xi^\alpha(\eta, \vec{x}) .
\tag{2.4}
$$

However, if we start in a gauge with only scalar perturbations, we can end up in a gauge with vector perturbations. These perturbations are, however, pure gauge, and thus of no interest. Such spurious gauge transformations can be avoided by limiting the gauge transformations of equation (2.4) to the form [38]

$$
\begin{aligned}
\tilde{\eta} &= \eta + \xi^0(\eta, \vec{x}) , \\
\tilde{x}^i &= x^i - \delta^{ij}\xi_{,j}(\eta, \vec{x}) .
\end{aligned}
\tag{2.5}
$$

To find out how the components of the metric transform under the gauge transformation of equation (2.5), one writes the expression for the line element ds^2 and

requires it to be invariant, i.e., of similar form to equation (2.3). This results in the transformation laws for the components of the metric perturbations:

$$\tilde{A} = A - \xi^{0\prime} - \frac{a'}{a}\xi^0 \tag{2.6}$$

$$\tilde{B} = B + \xi' + \xi^0 \tag{2.7}$$

$$\tilde{\psi} = \psi + \frac{a'}{a}\xi^0 \tag{2.8}$$

$$\tilde{E} = E + \xi \tag{2.9}$$

In the unperturbed FRW universe the energy momentum tensor reads

$$T^{\mu\nu} = (\rho + p)u^\mu u^\nu + p\,a^2\eta^{\mu\nu} \ , \tag{2.10}$$

where u^μ is the four-velocity of the fluid in the universe. Because the universe is isotropic, the four-velocity cannot have a spatial component, and thus $u^i = 0$. Furthermore since the norm of the vector must be $u_\mu u^\mu = -1$, the unperturbed velocity must be

$$u^\mu = (1/a, 0, 0, 0) \ .$$

If we add perturbations to the energy momentum tensor, it then reads

$$
\begin{aligned}
T^0_0 &= -\rho - \delta\rho \\
T^0_i &= (\rho + p)v_i \\
T^i_0 &= -(\rho + p)(v^i - B^{\cdot i}) \\
T^i_j &= \delta^i_j(p + \delta p) + \Sigma^i_j \ ,
\end{aligned}
$$

where Σ^i_j is the anisotropic stress tensor. Σ^i_j is gauge invariant, while the other perturbations are not, and they transform according to

$$\tilde{\delta\rho} = \delta\rho - \rho'\xi^0 \tag{2.11}$$

$$\tilde{\delta p} = \delta p - p'\xi^0 \tag{2.12}$$

$$\tilde{\delta q} = \delta q + (\rho + p)a\xi^0 \ . \tag{2.13}$$

Here δq is defined to be the momentum density, $\delta q_{,i} = (\rho + p)u_i$.

2.2 Gauge Invariant Combinations of the Perturbations

The scalar functions A, B, ψ and E specify the scalar perturbations of the metric. These functions are however gauge dependent, as is their evolution. Thus it would be more convenient to deal with gauge invariant quantities. Since we have four functions,

A, B, ψ and E, but two free functions defining the gauge, ξ^0 and ξ, we expect that there are two "physical" degrees of freedom. The separation into these two degrees of freedom is of course still arbitrary.

One choice of gauge invariant degrees of freedom are the so called *Bardeen potentials*, which are given by

$$\Phi_{\mathrm{B}} = A + \mathcal{H}(B - E') + (B - E')' \tag{2.14}$$
$$\Psi_{\mathrm{B}} = \psi - \mathcal{H}(B - E') . \tag{2.15}$$

By using the equations (2.6) - (2.9), it can be easily checked that Φ_{B} and Ψ_{B} are indeed gauge invariant.

Although Φ_{B} and Ψ_{B} are gauge invariant, they evolve in time non-trivially. Thus we define two other combinations of the scalar perturbations, which later on turn out to have interesting evolution for super-horizon modes. We first define the *curvature perturbation on uniform-density hypersurfaces* [39]

$$-\zeta = \psi + \frac{\mathcal{H}}{\rho'}\delta\rho . \tag{2.16}$$

The inspiration of the name of ζ is obvious: In a uniform-density gauge $\delta\rho = 0$, and ζ is just $-\psi$, and ψ in the non-relativistic limit is just the Newtonian potential. The minus sign is just an unfortunate relic of notation. We also define another gauge-invariant variable, the *comoving curvature perturbation* [40, 41]

$$\mathcal{R} = \psi - \frac{\mathcal{H}}{\rho + p}\delta q . \tag{2.17}$$

Since a comoving gauge is defined by $\delta q = 0$, in this gauge $\mathcal{R} = \psi$.

It can be shown that (see e.g. the computation in [18]) that the difference between $-\zeta$ and $\mathcal{R}$ is proportional to k^2,

$$\zeta + \mathcal{R} \propto \frac{k^2}{(aH)^2} ,$$

and thus, on large (superhorizon) scales $-\zeta$ and $\mathcal{R}$ coincide.

2.3   Evolution of the Perturbations

Until this point we have merely defined perturbed quantities. To find out how these quantities evolve dynamically, one has to use their equations of motion. In the context of general relativity, these are given by the Einstein equation (1.2), or

$$R_{\mu\nu} - \frac{1}{2}R\,g_{\mu\nu} = 8\pi G\,T_{\mu\nu} .$$

To find out the equations of motion for the perturbed quantities, one has to compute both the left hand side and the right hand side expressions in terms of the perturbations, and then expand the equation. To compute the LHS, one has to first calculate the connection coefficients

$$\Gamma^{\gamma}_{\alpha\beta} = \frac{1}{2} g^{\gamma\lambda} \left(\partial_\beta g_{\alpha\lambda} + \partial_\alpha g_{\beta\lambda} - \partial_\lambda g_{\alpha\beta} \right) ,$$

from which one then calculates the Riemann tensor

$$R^{\rho}{}_{\sigma\mu\nu} = \partial_\mu \Gamma^{\rho}_{\nu\sigma} - \partial_\nu \Gamma^{\rho}_{\mu\sigma} + \Gamma^{\rho}_{\mu\lambda} \Gamma^{\lambda}_{\nu\sigma} - \Gamma^{\rho}_{\nu\lambda} \Gamma^{\lambda}_{\mu\sigma}$$

and then contracts indices to get the Ricci tensor and scalar,

$$R_{\mu\nu} \equiv R^{\lambda}{}_{\mu\lambda\nu} \quad , \qquad R \equiv R^{\mu}_{\mu} .$$

This is straightforward, but quite laborous. Similarly one has to calculate the perturbations of the energy-momentum tensor $T_{\mu\nu}$. After this lengthy calculation one ends up with equation of motion for the different perturbations, describing their evolution.

We are interested however only in their super-horizon behaviour. In that case using only the local conservation of the energy-momentum tensor, $\nabla_\mu T^\mu_\nu = 0$, yields the result [42–44] on scales much larger than the horizon

$$\dot{\zeta} = -\frac{H}{\rho + p} \delta p_{\text{nad}} + \text{gradient terms} , \tag{2.18}$$

where p_{nad} is the non-adiabatic component of the pressure (see e.g. [45]). Indeed, by assuming the gradients to be small, we see that the curvature perturbation is conserved in super-horizon scales in the absence of non-adiabatic pressure. It is interesting to note that the conservation of the super-horizon perturbations follows directly from Poincaré symmetry of the underlying theory, and the form of the metric theory of gravitation is of no importance. Its form only governs the evolution of the sub-horizon modes.

The perturbation modes that we are interested in, that is those which are observable today, enter horizon long after inflation. These modes evolve according to Einstein equations, first linearly, but finally they form non-linear structures. The scope of the present work is to study the generation of these perturbations modes, and for that end their property that they are conserved while outside the horizon is sufficient.

2.4   The Power Spectrum

Consider a random variable $f(\mathbf{x}, t)$. We define the power spectrum of this variable by

$$\langle f_{\mathbf{k}} f^*_{\mathbf{k}'} \rangle = (2\pi)^3 \delta(\mathbf{k} - \mathbf{k}') \frac{2\pi^2}{k^3} \mathcal{P}_f(k) . \tag{2.19}$$

The reason for choosing the numerical prefactor $2\pi^2/k^3$, can be understood by considering the expectationg value of f^2 in real space. Since f is real in real space, we can write

$$
\begin{aligned}
\langle f^2(\mathbf{x}) \rangle &= \int \frac{\mathrm{d}^3\mathbf{k}}{(2\pi)^3} \int \frac{\mathrm{d}^3\mathbf{k}'}{(2\pi)^3} e^{i\mathbf{x}\cdot(\mathbf{k}-\mathbf{k}')} \langle f_\mathbf{k}\, f_{\mathbf{k}'}^* \rangle \\
&= \int \frac{\mathrm{d}^3\mathbf{k}}{(2\pi)^3} \frac{2\pi^2}{k^3} \mathcal{P}_f(k) \\
&= \int_0^\infty \mathrm{d}k\, \frac{\mathcal{P}_f(k)}{k} \,,
\end{aligned}
$$

thus $\mathcal{P}_f(k)$ is the contribution to the variance per unit logarithmic interval in the wavenumber k.

2.5 ΔN-formalism

Although first order perturbation theory appears to work extremely well in the early universe, certain features of interest, such as non-Gaussianity, would require the usage of second-order perturbation theory. This is very cumbersome, and often a non-perturbative alternative[2] is practical. The method described here is usually called the separate universe approach or ΔN-formalism [42, 46–51].

The metric can be written as [24, 50]

$$
\mathrm{d}s^2 = -\mathrm{d}t^2 + a^2(t)\, e^{-2\psi(t,\mathbf{x})} \mathrm{d}\mathbf{x}^2 \,,
$$

where $a(t)$ is the scale factor of the background solution.

Now consider two patches, a and b, at fixed spatial coordinates, separated by coordinate distance λ. The large-scale curvature perturbation can then be defined by

$$
\delta\psi = \psi_a - \psi_b \,,
$$

independent of the background. If we define the number of e-folds,

$$
N(t_2,t_1,\mathbf{x}) = \int_{t_1}^{t_2} \mathrm{d}t\, H(t,\mathbf{x}) \,,
$$

where $H(t,\mathbf{x})$ is now the actual Hubble parameter, not that of the background solution, then we can write

$$
\delta\psi(t) = N(t,t_0,\mathbf{x}_a) - N(t,t_0,\mathbf{x}_b) \,,
$$

---

[2]The ΔN-formalism is a zeroth-order gradient expansion, and thus actually a perturbative method. Anyhow, since the expansion is not done in the curvature perturbation, and thus encompasses it to all orders, this is often called non-perturbative.

or essentially

$$-\zeta = \Delta N \ .$$

Thus we can compute the evolution of the curvature perturbation by comparing the number e-folds of two patches with initial conditions corresponding to the initial perturbation.

The evolution of these separate patches is in principle non-trivial, and should be computed. Indeed the equation of motion for the patches can be calculated and shown to coincide with the background equation of motion in a gradient expanson to first order [24]. A more elegant argument is however given by Wands et al. [42]: There has to be *some* scale λ_s for which the assumption that the separate patches evolve as if independent background solutions, since if there were not, the concept of unperturbed Friedmann-Robertson-Walker universe would make no sense. By background we mean an even larger scale, λ_0, with respect to which we define our perturbations. Thus we actually require a hierarchy of scales,

$$\lambda_0 \gg \lambda \gg \lambda_s \ ,$$

which merely states the fact that we assume that the universe is homogeneous on very large scales, that we are interested in perturbations which are of smaller scale, and that the evolution of these perturbations is independent of shorter wavelength perturbations.

The ΔN formalism is very suitable for calculating, for example, non-Gaussianity parameters, since ΔN incorporates all orders of ζ. It is also very suitable to numerics, since the problem of solving the evolution of perturbations is reduced to solving the background equations with different initial conditions.

Chapter 3

Generating Perturbations

Inflationary models, including the curvaton model which is the main topic of this thesis, have the general property that they are capable of producing the primordial perturbations that we observe in the CMB and which seed all structure in the universe. This amazing property is due to quantum fluctuations in the expanding universe: The quantum fluctuations of a scalar field on scales much smaller than the horizon become larger and larger as the universe expands, until they cross the horizon and become classical perturbations of the field.

3.1   Quantizing a Scalar Field in de Sitter Space

We are interested in calculating the expectation value of quantum fluctuations of a field. To do this, we need to quantize a scalar field in curved background. This proceeds in analogy with the quantization of scalar fields in flat space-time. Since the background is time dependent, the computation is easiest to perform using canonical quantization. The procedure is the following:

1. Write the action and derive the equation of motion from that.

2. Find the mode functions by solving the equation of motion.

3. Promote the field and its canonical momentum to operators. Write the field operator by using ladder operators and the mode functions, and find the proper normalization for the mode functions by requiring that the operators obey the canonical commutation relations.

4. Calculate the expectation value of the field correlator.

We start out with a scalar field in de Sitter space,

$$S = \int \mathrm{d}^4 x \, \sqrt{-g} \left[-\frac{1}{2} \partial_\mu \phi \, \partial^\mu \phi - V(\phi) \right] ,$$

where the metric is given by

$$ds^2 = -dt^2 + a(t)^2 d\mathbf{x}^2 \quad , \quad a(t) \propto e^{Ht} .$$

Since the determinant of the metric is $g = -a^6$ and $dt = d\eta \, a$, the action can be rewritten in conformal time to be

$$S = \frac{1}{2} \int d^3\mathbf{x} \, d\eta \, a^2 \left[\phi'^2 - (\nabla\phi)^2 - 2a^2 V(\phi) \right] .$$

Using the Euler-Lagrange equations, we find the equation of motion to be

$$\phi'' + 2\mathcal{H}\phi' - \nabla^2\phi + a^2 m^2 \phi = 0 . \tag{3.1}$$

To get rid of the single time derivative in equation (3.1), we introduce a new variable $\tilde{\phi} \equiv a\phi$. Subsituting this definition into equation (3.1) and multiplying by a, we get the equation of motion for $\tilde{\phi}$ to be

$$\tilde{\phi}'' + \left(-\nabla^2 - \mathcal{H}' - \mathcal{H}^2 + a^2 m^2 \right)\tilde{\phi} = 0 .$$

To find the mode functions $u_\mathbf{k}$ of $\tilde{\phi}$ we take the Fourier transform of the equation so that $\nabla \to -ik$, and use the fact that since in de Sitter space-time $H = $ const, $\mathcal{H} = -1/\eta$ and $a = -1/H\eta$. Then the equation for the mode functions is given by

$$u_k'' - \frac{2}{\eta^2} u_k + k^2 u_k + \frac{m^2}{H^2 \eta^2} u_k = 0 .$$

This is in fact a Bessel equation,

$$u_k'' + \left(k^2 - \frac{v^2 - \frac{1}{4}}{\eta^2} \right) u_k = 0 , \tag{3.2}$$

with the index

$$v^2 = \frac{9}{4} - \frac{m^2}{H^2} .$$

When v is real, equation (3.2) has the solution [30, 52]

$$u_k(\eta) = \sqrt{-\eta} \left[c_1(k) \, H_v^{(1)}(-k\eta) + c_2(k) \, H_v^{(2)}(-k\eta) \right] , \tag{3.3}$$

where $H_v^{(1)}$ and $H_v^{(2)}$ are the Hankel functions of first and second kind.

The solution in equation (3.3) has two arbitrary coefficients c_1 and c_2. The freedom in choosing those coefficients corresponds to the freedom of choosing a vacuum. Thus a problem arises from the fact that in quantum field theory in curved space the choice of vacuum is no longer unique: A state which has zero particle number at a given time has generally a non-zero particle number in some other time. This can be

considered to be a result of the non-trivial time evolution of the background space-time. This feature is also responsible for the phenomenon we are interested in, that is, inflationary space time producing particles, i.e., excitations of the field. To choose a vacuum, we need to specify *which* vacuum is the one we are interested in. In general this is a very fundamental problem of quantum fields in curved space, however, in this case we have a very natural choice of vacuum: we simply require that in the ultraviolet limit, $k \gg aH$ and $k \gg m$, the mode functions match the solutions of Minkowski space, so that the choice of vacuum coincides with our "intuitive" notion of vacuum[1],

$$u_k \to \frac{1}{\sqrt{2k}} e^{-ik\eta} \ . \tag{3.4}$$

Using the formulas for the asymptotic behaviour of the Hankel functions,

$$H_\nu^{(1)}(x \gg 1) \sim \sqrt{\frac{2}{\pi x}} e^{i\left(x - \frac{\pi}{2}\nu - \frac{\pi}{4}\right)} \quad , \quad H_\nu^{(2)}(x \gg 1) \sim \sqrt{\frac{2}{\pi x}} e^{-i\left(x - \frac{\pi}{2}\nu - \frac{\pi}{4}\right)} \ ,$$

we are lead to $c_1(k) = \frac{\sqrt{\pi}}{2} e^{i\left(\nu + \frac{1}{2}\right)\frac{\pi}{2}}$ and $c_2(k) = 0$. Thus the mode functions are given by

$$u_k(\eta) = \frac{\sqrt{\pi}}{2} e^{i\left(\nu + \frac{1}{2}\right)\frac{\pi}{2}} \sqrt{-\eta} \, H_\nu^{(1)}(-k\eta) \ . \tag{3.5}$$

To quantize the field $\tilde{\phi}$, we promote the field to an operator, and expand it in terms of the mode functions and ladder operators:

$$\tilde{\phi} = \int \frac{d^3 \mathbf{k}}{(2\pi)^3} \left[u_{\mathbf{k}}(\eta) \, \hat{a}_{\mathbf{k}} \, e^{i\mathbf{k}\cdot\mathbf{x}} + u_{\mathbf{k}}^*(\eta) \, \hat{a}_{\mathbf{k}}^\dagger \, e^{-i\mathbf{k}\cdot\mathbf{x}} \right] \ . \tag{3.6}$$

Then we impose the canonical commutation relations for $\tilde{\phi}$ and its canonical momentum $\tilde{\pi}$,

$$[\tilde{\phi}(\mathbf{x}), \tilde{\pi}(\mathbf{y})] = i\delta(\mathbf{x} - \mathbf{y})$$
$$[\tilde{\phi}(\mathbf{x}), \tilde{\phi}(\mathbf{y})] = [\tilde{\pi}(\mathbf{x}), \tilde{\pi}(\mathbf{y})] = 0 \ .$$

These relation give familiar relations for the ladder operators $\hat{a}_{\mathbf{k}}$ and $\hat{a}_{\mathbf{k}}^\dagger$,

$$[a_{\mathbf{k}}, a_{\mathbf{k}'}^\dagger] = (2\pi)^3 \delta(\mathbf{k} - \mathbf{k}') \ .$$

Also we get the normalization condition for the mode functions to be

$$u_k^* u_k' - u_k u_k^{*\prime} = -i \ , \tag{3.7}$$

which the mode functions obey, since we chose the normalization for the mode functions in equation (3.4) serendipitously.

---

[1]The normalization at this point is in principle arbitrary. However, the normalization in equation (3.4) has been chosen so that the normalization condition in equation (3.7) is satisfied.

Next we can calculate the expectation value of the correlator. We do this in momentum space,

$$
\begin{aligned}
\langle \tilde{\phi}_{\mathbf{k}}^{\dagger} \tilde{\phi}_{\mathbf{k}'} \rangle &= \left\langle \left(u_{\mathbf{k}}^{*} \hat{a}_{\mathbf{k}}^{\dagger} + u_{\mathbf{k}} \hat{a}_{\mathbf{k}} \right) \left(u_{\mathbf{k}'} \hat{a}_{\mathbf{k}'} + u_{\mathbf{k}'}^{*} \hat{a}_{\mathbf{k}'}^{\dagger} \right) \right\rangle \\
&= \left\langle u_{\mathbf{k}} u_{\mathbf{k}'}^{*} \hat{a}_{\mathbf{k}} \hat{a}_{\mathbf{k}'}^{\dagger} \right\rangle \\
&= (2\pi)^{3} \delta(\mathbf{k} - \mathbf{k}') \, u_{\mathbf{k}} u_{\mathbf{k}}^{*} \; .
\end{aligned}
$$

To calculate the correlator of the original field ϕ we simply divide by a^2,

$$
\langle \phi_{\mathbf{k}}^{\dagger} \phi_{\mathbf{k}'} \rangle = \frac{\langle \tilde{\phi}_{\mathbf{k}}^{\dagger} \tilde{\phi}_{\mathbf{k}'} \rangle}{a^{2}(\eta)} = (2\pi)^{3} \delta(\mathbf{k} - \mathbf{k}') \frac{\pi}{4} \frac{-\eta}{a^{2}(\eta)} \left[H_{\nu}^{(1)}(-k\eta) \right]^{2} \; .
$$

This correlator has explicit time dependence. However, we are interested in the behaviour of superhorizon modes in the massless limit. Thus taking the superhorizon limit $|k\eta| \ll 1$, and using the asymptotic limit for the Hankel functions,

$$
H_{\nu}^{(1)}(x \ll 1) \sim \sqrt{\frac{2}{\pi}} e^{-i\frac{\pi}{2}} 2^{\nu - \frac{3}{2}} \frac{\Gamma(\nu)}{\Gamma(3/2)} x^{-\nu} \; ,
$$

we can write

$$
\langle \phi_{\mathbf{k}}^{\dagger} \phi_{\mathbf{k}'} \rangle = (2\pi)^{2} \delta(\mathbf{k} - \mathbf{k}') \frac{-\eta}{a^{2}(\eta)} 2^{2\nu - 4} \left[\frac{\Gamma(\nu)}{\Gamma(\frac{3}{2})} \right]^{2} (-k\eta)^{-2\nu}
$$

In the massless limit, $\nu \to \frac{3}{2}$, this reads

$$
\langle \phi_{\mathbf{k}}^{\dagger} \phi_{\mathbf{k}'} \rangle = (2\pi)^{3} \delta(\mathbf{k} - \mathbf{k}') \frac{1}{2 \, a^{2}(\eta) \, k^{3} \eta^{2}} \; .
$$

Using the fact that in de Sitter space $a(\eta) = -1/H\eta$, this reduces to

$$
\langle \phi_{\mathbf{k}}^{\dagger} \phi_{\mathbf{k}'} \rangle = (2\pi)^{3} \delta(\mathbf{k} - \mathbf{k}') \frac{H^{2}}{2k^{3}} \; . \tag{3.8}
$$

Comparing this with equation (2.19) we get the expression for the power spectrum of the field,

$$
\mathcal{P}_{\phi} = \left(\frac{H}{2\pi} \right)^{2} \; ,
$$

demonstrating that massless fields aquire scale-invariant perturbations in de Sitter space for modes that have exited the horizon.

3.2   Scaling Solutions for Oscillating Fields

Once the perturbations are created, we need to know how different energy components in the early universe evolve. For a field undergoing sufficiently fast coherent oscillations in an expanding background, there exists a simple scaling law for the energy density of the field. Following Turner [53], we now derive this scaling law.

Assume that a field is oscillating around its miniumum in a symmetric potential $V(\phi)$. The energy density and pressure are given by

$$\rho = \frac{1}{2}\dot{\phi}^2 + V(\phi)$$

$$p = \frac{1}{2}\dot{\phi}^2 - V(\phi) .$$

As the field value ϕ oscillates, so do ρ and p. If the oscillations are fast enough,

$$\omega \simeq \dot{\phi}/\phi \gg H , \tag{3.9}$$

we can divide the evolution of the field into two separate components,

$$(\gamma + \gamma_p)\rho = \rho + p , \tag{3.10}$$

where γ is the average over one oscillation, and is thus the evolution of the *envelope* of the oscillation, and γ_p is the term describing the (nearly) sinusoidal oscillation. Note that from this it follows that γ_p averaged over one oscillation is zero.

The equation of motion for the field

$$\ddot{\phi} + 3H\dot{\phi} + V'(\phi) = 0$$

can be rewritten to be as an equation for the energy density,

$$\dot{\rho} = -3H(\rho + p) .$$

Substituting equation (3.10) into this, and integrating, we get

$$\ln \frac{\rho}{\rho_0} = -3\left(\int dt \, \frac{\dot{a}}{a}\gamma + \int dt \, \frac{\dot{a}}{a}\gamma_p \right) .$$

The latter term goes to zero as the oscillations becomes faster, due to γ_p averaging to zero over an oscillation cycle. If γ is constant, then the first term can be readily integrated to give

$$\rho = \rho_0 \left(\frac{a}{a_0} \right)^{-3\gamma} . \tag{3.11}$$

The expression for γ can be derived by averaging equation (3.10) over one cycle of oscillation. Since the oscillation period is very short, we can approximate the energy density to be fixed, $\rho \simeq V(\phi_{\max})$. Writing $\rho + p = \dot{\phi}^2$ we get

$$\int_{t_1}^{t_2} dt \, \dot{\phi}^2 = V(\phi_{\max}) \int_{t_1}^{t_2} dt \, (\gamma + \gamma_p) .$$

Here the integral over γ_p is by definition zero, and can be omitted.

Since the potential is symmetric, instead of integrating over a full oscillation, we can integrate over a quarter of it, from 0 to ϕ_{max}. Changing the integration limits, as well changing the integration variable from t to ϕ, gives for constant γ

$$\gamma = \frac{\displaystyle\int_0^{\phi_{max}} d\phi \, \dot{\phi}}{V(\phi_{max}) \displaystyle\int_0^{\phi_{max}} d\phi \, \dot{\phi}^{-1}} \; .$$

Now since $\frac{1}{2}\dot{\phi}^2 = \rho - V(\phi)$, we can substitute $\dot{\phi}$ to give the expression for γ:

$$\gamma = 2 \frac{\displaystyle\int_0^{\phi_{max}} d\phi \left[1 - \frac{V(\phi)}{V(\phi_{max})} \right]^{\frac{1}{2}}}{\displaystyle\int_0^{\phi_{max}} d\phi \left[1 - \frac{V(\phi)}{V(\phi_{max})} \right]^{-\frac{1}{2}}} \tag{3.12}$$

Now consider a monomial potential,

$$V(\phi) = \lambda \phi^n \; .$$

Substituting this into equation (3.12), we get

$$\gamma = 2 \frac{\displaystyle\int_0^1 dx \, \sqrt{1 - x^n}}{\displaystyle\int_0^1 dx \, \frac{1}{\sqrt{1 - x^n}}} \; .$$

The two integrals can be integrated easily by changing variables $x^n \to y$, giving a fraction of Euler beta functions,

$$\gamma = \frac{\frac{1}{n} \displaystyle\int_0^1 dy \, y^{\frac{1}{n}-1}(1 - y)^{\frac{1}{2}}}{\frac{1}{n} \displaystyle\int_0^1 dy \, y^{\frac{1}{n}-1}(1 - y)^{-\frac{1}{2}}} = \frac{2n}{n + 2} \; .$$

Inserting this value for γ in equation (3.11), we get the following expressions for different powers of the potential $V \propto \phi^n$:

$$\begin{aligned}
n &= 2: & \rho &\propto a^{-3} \text{, dilutes like cold matter} \\
n &= 4: & \rho &\propto a^{-4} \text{, dilutes like radiation} \\
n &\geq 6: & \rho &\text{ dilutes faster than radiation}
\end{aligned} \tag{3.13}$$

The preceding calculation was based on the assumption that the field was oscillating rapidly in a monomial potential. For large values of n, specifically $n \geq 10$, the field no longer has oscillatory solutions, but rather only decaying modes, and thus the above calculation is inapplicable. Nevertheless, the decaying mode for $n \geq 10$ has a scaling law with similar behaviour.

3.3 Slow-roll Inflation

In the first section of this chapter we computed the spectrum of perturbations that a free scalar field acquires in de Sitter space. The idea in inflation generating primordial perturbations is that the perturbations in the inflaton field are transformed into perturbations of the energy density or — depending on the gauge choice — curvature of space. To compute the spectrum of those perturbations we need to relate the perturbations of the scalar field to the curvature perturbations, namely $\mathcal{R}$.

In spatially flat gauge, $\psi = 0$, the comoving curvature perturbation of equation (2.17) reads

$$\mathcal{R} = -\frac{\mathcal{H}}{\rho + p}\delta q \ .$$

Here δq is defined by $T_i^0 \equiv \partial_i \delta q$. Assuming that inflation is driven by a scalar field φ, with the Lagrangian density

$$\mathcal{L} = -\partial_\mu \varphi\, \partial^\mu \varphi - V(\varphi) \ ,$$

we can compute the energy-momentum tensor from

$$T_{\mu\nu} = \frac{\partial \mathcal{L}}{\partial(\partial^\mu \varphi)}\partial_\nu \varphi - g_{\mu\nu}\mathcal{L} \ .$$

This yields

$$T_i^0 = -\partial^0 \overline{\varphi}\, \partial_i \delta\varphi + \mathcal{O}(\delta\varphi^2) \ ,$$

from which we can read off $\delta q = -(\partial^0 \overline{\varphi})\delta\varphi$. Here the overbar denotes the unperturbed background value. On the other hand using equation (1.7) we can write $\rho + p = (\partial^0 \varphi)^2$, so that the comoving curvature perturbation reads

$$\mathcal{R} = \mathcal{H}\frac{\delta\varphi}{\varphi'} = H\frac{\delta\varphi}{\dot{\varphi}} \ . \tag{3.14}$$

Here the second equality follows from using the identities $\dot{f} = f'/a$ and $H = \mathcal{H}/a$.

Using equation (3.14) we can express the correlator of the curvature perturbation in terms of the correlator of the perturbation of the scalar field,

$$\langle \mathcal{R}_{\mathbf{k}} \mathcal{R}_{\mathbf{k}'} \rangle = \left(\frac{H}{\dot{\varphi}}\right)^2 \langle \delta\varphi_{\mathbf{k}}\delta\varphi_{\mathbf{k}'} \rangle \ ,$$

or, in terms of the power spectrum,

$$\mathcal{P}_{\mathcal{R}}(k) = \left(\frac{H}{\dot{\varphi}}\right)^2 \mathcal{P}_{\delta\varphi}(k) \,.$$

In the context of *slow-roll* inflation, we assume that the inflaton field φ is homogeneous and slowly varying. Furthermore, since we assume that the field sits still for a period long enough, the field must be in a point in the potential where the curvature is very small. Thus the perturbation of the field, $\delta\varphi$, is effectively massless. This means that $\mathcal{P}_{\delta\varphi}(k)$ is given by equation (3.8), and thus

$$\mathcal{P}_{\mathcal{R}}(k) = \left(\frac{H}{\dot{\varphi}}\right)^2 \left(\frac{H}{2\pi}\right)^2 \,.$$

Often the results for slow-roll inflation are expressed in terms of the slow-roll parameters ε and η. Using the slow-roll approximation $\dot{\varphi} \simeq -V'/3H$, we can write

$$\mathcal{P}_{\mathcal{R}}(k) = \left(\frac{3H^2}{V'}\right)^2 \left(\frac{H}{2\pi}\right)^2 \,.$$

Since the energy density of the universe is dominated by the potential energy of the inflaton field, $3H^2 M_{\mathrm{Pl}}^2 \simeq V(\varphi)$, and then using the definitions of the slow-roll parameters given in equations (1.8) and (1.9), we can write

$$
\begin{aligned}
\mathcal{P}_{\mathcal{R}}(k) &= \left(\frac{3H^3}{V'2\pi}\right)^2 = \left(\frac{3H^2 M_{\mathrm{Pl}}^2}{V'}\frac{H}{2\pi M_{\mathrm{Pl}}}\right)^2 \\
&= \left(\frac{V}{V'}\right)^2 \left(\frac{H}{2\pi M_{\mathrm{Pl}}}\right)^2 \\
&= \frac{M_{\mathrm{Pl}}^2}{2\varepsilon}\frac{H^2}{(2\pi)^2 M_{\mathrm{Pl}}^4} = \frac{V}{24\pi^2 M^4}\frac{1}{\varepsilon} \,.
\end{aligned}
$$

Since the amplitude of $\mathcal{P}_{\mathcal{R}}(k)$ is fixed, i.e., the COBE normalization is given in equation (1.10), this means that the slow-roll parameter ε and the value of the potential at the point of inflation must be tuned to produce the observed amplitude of perturbations.

The Spectral Index

Even though the field is in slow-roll, the perturbation spectrum is not completely scale-invariant. In principle the spectrum might have arbitrary behavior over a large range of wave-numbers k. In practice, however, the primordial perturbations are observed only for a limited window of k, corresponding to the range of scales observable in the CMB and in large scale structure. In that limited range the spectrum has been

observed to be nearly scale invariant, and thus it is common to parametrize the scale-dependence in the spectrum by a single number, *the spectral index*, defined by

$$\frac{d\ln\mathcal{P}_\mathcal{R}(k)}{d\ln k} \equiv n_s - 1 \ . \tag{3.15}$$

Since n_s is without scale dependence, the above definition should be considered to apply at some fixed scale k_{ref}.

Since the perturbations do not evolve after they have stretched to be larger than the horizon, we can evaluate them at horizon exit, $k = aH$. Thus we can exchange the differentation with respect to k to a differentiation with respect to time,

$$\frac{d}{d\ln k} = \frac{dt}{d\ln k}\frac{d}{dt} = \frac{1}{H}\frac{d}{dt} + \mathcal{O}(\varepsilon) \ .$$

We can then first differentiate the slow-roll parameter ε,

$$\begin{aligned}
\frac{d\varepsilon}{d\ln k} &= \frac{1}{H}\frac{d}{dt}\frac{M_{\text{Pl}}^2}{2}\left(\frac{V'}{V}\right)^2 \\
&= \frac{M_{\text{Pl}}^2}{H}\dot{\varphi}\left(\frac{V'V''}{V^3} - \frac{V'^3}{V^3}\right) \\
&= -\frac{M_{\text{Pl}}^2}{3H^2}\left(\frac{V'V''}{V^3} - \frac{V'^3}{V^3}\right) \\
&= -M_{\text{Pl}}^4\left[\left(\frac{V'}{V}\right)^2\frac{V''}{V} - \left(\frac{V'}{V}\right)^4\right] \\
&= 4\varepsilon^2 - 2\eta\varepsilon \ ,
\end{aligned}$$

where we have again used the slow-roll approximations $\dot{\varphi} \simeq -V'/3H$ and $3H^2 M_{\text{Pl}}^2 \simeq V$ and ignored higher order terms. Using the above results it is straightforward to calculate

$$\begin{aligned}
\frac{d\ln\mathcal{P}_\mathcal{R}(k)}{d\ln k} &= \frac{1}{H}\frac{V'}{V}\dot{\varphi} - \frac{1}{\varepsilon}\frac{d\epsilon}{d\ln k} \\
&= \frac{1}{H}\frac{V'}{V}\left(\frac{-V'}{3H}\right) - \frac{1}{\varepsilon}\frac{d\epsilon}{d\ln k} \\
&= -2\varepsilon - \frac{1}{\varepsilon}\left(4\varepsilon^2 - 2\eta\varepsilon\right) = 2\eta - 6\varepsilon \ ,
\end{aligned}$$

so that the spectral index is given by

$$n_{\text{s}} = 1 + 2(\eta - 3\varepsilon) \ .$$

The best observational bounds on the spectral index, combining different datasets [13], give

$$n_{\text{s}} = 0.963 \pm 0.012 \ .$$

3.4 The Curvaton Scenario

In inflation the inflaton field acquires perturbations which are then translated to a curvature perturbation during reheating. The computation of section 3.1 nevertheless applies to any scalar field in de Sitter space-time. Thus *any* massless field can acquire nearly scale-invariant perturbations. In *the curvaton scenario* [54–58] the primordial perturbations originate not from the inflaton, but from quantum fluctuations of another scalar field, which has negligible energy density during inflation.

During inflation the curvaton field, σ, has some homogeneous background value, σ_*. Even if the initial configuration for σ is not homogeneous, inflation will quickly erase all inhomogeneities. On top of the homogeneous background value, σ will acquire perturbations originating from quantum fluctuations. If the field is light enough, $m_\sigma \ll H$, the magnitude of the perturbations is given by the calculation in section 3.1,

$$\delta\sigma \simeq \frac{H_*}{2\pi} \ .$$

After inflation ends, the inflaton decays into radiation, so that the universe becomes radiation dominated. While the radiation component initially dominates the energy density of the universe, it scales as

$$\rho_{\mathrm{r}} \propto a^{-4} \ ,$$

with the Hubble scale decreasing as

$$H = \sqrt{\frac{\rho_{\mathrm{r}*}}{3}} \frac{1}{M_{\mathrm{Pl}}} \left(\frac{a_*}{a}\right)^2 \ .$$

The curvaton, instead, evolves according to the shape of its potential. Initially the curvaton field is in slow-roll, $V'' \ll H^2$, during which the value of the field stays constant. Once the Hubble friction no longer dominates and the curvaton exits slow-roll, it starts to oscillate around the minimum of its potential. During these oscillations, the scaling behaviour of its energy density depends on the power of the potential, as described in section 3.2. In the simplest curvaton model the potential is quadratic, so according to the calculation of section 3.2,

$$\rho_\sigma \propto a^{-3} \ .$$

Thus the fraction of total energy density contributed by the curvaton increases as a function of time, until it starts to initially contribute significantly to, and finally dominate, the energy density of the universe. The curvaton then decays into the radiation degrees of freedom.

The perturbations in the curvaton field are initially a mixture of adiabatic and isocurvature perturbations, but when the curvaton decays into radiation, the perturbations are transformed into adiabatic ones. The transformation is due to the decay

of the curvaton field: Since there is a single degree of freedom (radiation density) left, there can be no isocurvature perturbations. In principle the final perturbations might be a mixture of perturbations originating from the curvaton and the inflaton [56, 59–64], or possibly multiple curvatons [65, 66].

In analogy with the definition of ζ in equation (2.16) we can define ζ for multiple fluid components. In spatially flat gauge ($\psi = 0$) the definition of ζ reads

$$-\zeta = \frac{\mathcal{H}}{\rho'}\delta\rho \ .$$

The interpretation of this is simply that the perturbation is a perturbation of the energy density of fluid. If we have multiple fluid components, we can analogously define perturbation for each component separately,

$$-\zeta_i = \frac{\mathcal{H}}{\rho_i'}\delta\rho_i \ .$$

In the case which is relevant here, we have two components: radiation, and the curvaton, which scales like matter. Remembering the scaling laws of equation (3.13), we thus get

$$\zeta_\sigma = \frac{1}{3}\frac{\delta\rho_\sigma}{\rho_\sigma}$$
$$\zeta_{\mathrm{r}} = \frac{1}{4}\frac{\delta\rho_{\mathrm{r}}}{\rho_{\mathrm{r}}} \ .$$

Using these definitions to write the total perturbation, we get

$$\zeta = -\mathcal{H}\frac{\sum_i \delta\rho_i}{\sum_i \rho_i'} = \frac{3\rho_\sigma\zeta_\sigma + 4\rho_{\mathrm{r}}\zeta_{\mathrm{r}}}{3\rho_\sigma + 4\rho_{\mathrm{r}}} \ .$$

We are interested in the case where only the curvaton produces perturbations, so we write

$$\zeta = \frac{3\rho_\sigma\zeta_\sigma}{3\rho_\sigma + 4\rho_{\mathrm{r}}} \ .$$

Since the perturbation becomes adiabatic only after the curvaton decays, and assuming that the decay is instantaneous [67], we should evaluate the perturbation at decay. Thus we write

$$\zeta = \left.\frac{3\rho_\sigma\zeta_\sigma}{3\rho_\sigma + 4\rho_{\mathrm{r}}}\right|_{\mathrm{decay}} \equiv r_{\mathrm{dec}}\,\zeta_\sigma \ , \tag{3.16}$$

where we have defined the efficiency factor r_{dec}.

To proceed with the analysis of the curvaton model we need to know the value of ζ_σ when the curvaton decays. To compute this, we use the fact that if the potential of the curvaton field is quadratic, then both the homogeneous background field and

the perturbation of the curvaton field obey the same equation of motion, and thus, the relative perturbation in the curvaton field stays constant. Indeed, this can be seen by comparing with equation (2.18). Using the definition of δp_{nad} [45] to compute it for a field undergoing quadratic oscillations

$$\delta p_{\mathrm{nad}} = \dot{\varphi}\, \delta\dot{\varphi} - m^2\, \varphi\, \delta\varphi = 0,$$

where the last equality follows from the sinusoidal form of the oscillations, we can conclude that for a quadratic field the non-adiabatic pressure is zero, and thus the perturbation stays constant for super-horizon modes. Thereby ζ_σ is related to the initial conditions by simply

$$\zeta_\sigma = \frac{1}{3}\frac{\delta\rho_\sigma}{\rho_\sigma} \simeq \frac{1}{3}\frac{\rho_\sigma'(\sigma_*)\delta\sigma_*}{\rho_\sigma(\sigma_*)} = \frac{H_*}{3\pi\sigma_*}\;,$$

where the prime denotes a derivative with respect to σ. Inputting this to equation (3.16), we get the final expression for the perturbation produced by a curvaton with a quadratic potential,

$$\zeta = \frac{r_{\mathrm{dec}} H_*}{3\pi\sigma_*}\;. \tag{3.17}$$

In the limit that the curvaton is completely dominant when it decays, $r_{\mathrm{dec}} \to 1$, and

$$\zeta = \frac{H_*}{3\pi\sigma_*}\;.$$

In the limit that the curvaton is very subdominant when it decays, $r_{\mathrm{dec}} \ll 1$, and

$$\zeta = \frac{H_*}{4\pi\sigma_*}\left.\frac{\rho_\sigma}{\rho_{\mathrm{r}}}\right|_{\mathrm{decay}}\;.$$

Note that in the limit where r_{dec} is very small, $\delta\sigma_*/\sigma_*$ becomes larger and larger, and the applicability of linear perturbation theory is questionable. In practice, however, the cases where r_{dec} is very small are ruled out by large non-Gaussianity for quadratic models, as we will see in chapter 4.

Chapter 4

Non-Gaussianity of the Primordial Perturbations

For a Gaussian random field, $\phi(\mathbf{x})$, all statistical quantities are encoded in the *two-point correlation function*

$$\langle \phi(\mathbf{x})\phi(\mathbf{y}) \rangle \ .$$

All even higher order correlation functions are then given by just products of the two-point correlation function, while all odd higher order correlation functions are zero, and we say that the *connected part* of the higher order correlation functions are zero.

In Fourier space the two point correlation function is given by equation (2.19), and thus all information about the distribution of the random field encoded in the two-point correlation function is usually expressed using the power spectrum, $\mathcal{P}(k)$.

The observations of the primordial perturbations, mainly through the CMB, have indicated them to be highly Gaussian. Some deviations from complete Gaussianity can be however expected. To quantify these deviations, non-linearity, or non-Gaussianity, parameters f_{NL} and g_{NL} are usually used. These are defined by expanding the perturbation around a Gaussian distribution [68–70],

$$\zeta = \zeta_1 + \frac{3}{5}f_{\mathrm{NL}}\zeta_1^2 + \frac{9}{25}g_{\mathrm{NL}}\zeta_1^3 + \mathcal{O}(\zeta_1^4) \ . \tag{4.1}$$

The numerical prefactors in the definition of f_{NL} and g_{NL} are due to the early convention of characterising the primordial perturbations by the metric potential in the matter-dominated era, $\Phi = \frac{3}{5}\zeta$.

The expansion in equation (4.1) of course makes sense only in the case when we know that the distribution is close to Gaussian, and thus the use of this form is justified from the observations of the perturbations.

The non-Gaussianity parameters f_{NL} and g_{NL} measure the strength of the *bispectrum* and *trispectrum* respectively. The bispectrum corresponds to the connected part

of a 3-point function and the trispectrum to the connected part of a 4-point function. In principle one could define even higher order non-Gaussianity parameters, quad-spectrum, pentaspectrum etc., which would measure the non-Gaussianity of higher n-point correlators. However, since ζ is very small, the magnitude of n-point correlators becomes increasingly small as n increases. Already $\zeta^2 \sim 10^{-10}$, and $\zeta^3 \sim 10^{-15}$. For this reason, most work in non-Gaussianity is concentrated only on $f_{\rm NL}$ and $g_{\rm NL}$ [71, 72].

Note that in equation (4.1) the products between the non-Gaussianity parameters and the powers of ζ should in principle be a convolution over momentum space, since the non-Gaussianity is *a priori* momentum dependent. Indeed, the scale dependence of $f_{\rm NL}$ has been recently studied in [73, 74], and also for curvaton models [75]. In spite of that we consider only scale independent non-Gaussianity, also called *local* non-Gaussianity, for the rest of this work.

Best current bounds on the values of the non-Gaussianity parameters come from the CMB, and are given by [31] and [76],

$$-9 < \quad f_{\rm NL} \quad < 111 \qquad , \tag{4.2}$$

$$-3.5 \times 10^5 < \quad g_{\rm NL} \quad < 8.2 \times 10^5 \qquad . \tag{4.3}$$

As can be seen, the limits on $g_{\rm NL}$ are much less strict. This is to be expected, since the trispectrum is five orders of magnitude smaller then the bispectrum. Future CMB experiments are expected to be able to detect much smaller values of the non-Gaussianity parameters. For example, the Planck surveyor mission [77] is expected to reduce the limits of $f_{\rm NL}$ by almost an order of magnitude.

The value of $f_{\rm NL}$ can also be measured from the large scale structure of the universe. This corresponds to measuring the distribution of galaxies in the older universe, and then extrapolating backwards in time to figure out the primordial density perturbations. This method can give almost as good limits, for example [78] $-29 < f_{\rm NL}^{\rm local} < 70$.

It is noteworthy that if $f_{\rm NL} \sim \mathcal{O}(100)$ and $g_{\rm NL} \sim f_{\rm NL}^2$, the expansion of equation (4.1) might not seem good at first glance since the parameters are much larger than one. However, the parameter in which the expansion is done is ζ, which is very small, $\sim 10^{-5}$. Thus the ratio between the second order term and the first order term in the expansion is of order 10^{-3}.

4.1 Non-Gaussianity in the ΔN-formalism

If the primordial perturbation is sourced by a single field,[1] φ, then we can expand ΔN around the initial background value of the field φ_*,

$$\zeta = \Delta N = N'(\varphi_*)\delta\varphi_* + \frac{1}{2}N''(\varphi_*)\delta\varphi_*^2 + \frac{1}{6}N'''(\varphi_*)\delta\varphi_*^3 + \mathcal{O}(\delta\varphi_*^4) , \tag{4.4}$$

---

[1]In fact, nothing limits the notation for a single field: If the perturbation is sourced by two fields, then we might just as well expand $\Delta N = N_\sigma \delta\sigma + N_\varphi \delta\varphi + \frac{1}{2}N_{\sigma\sigma}\delta\sigma^2 + \frac{1}{2}N_{\sigma\varphi}\delta\sigma\delta\varphi + \frac{1}{2}N_{\varphi\varphi}\delta\varphi^2 + \ldots$

where the prime now denotes a derivative with respect to φ. When calculating ΔN, the number of e-folds in both patches are to be evaluated from the initial slice to a constant energy density slice where the universe is dominated by radiation. Thus the derivative denoted by prime is to be calculated with the additional condition that the energy density of the final slice stays constant. For a two-component fluid, this complication must be kept in mind.

If $\delta\varphi_*$ is small, we can identify order by order the perturbations of the above equation with the perturbations of equation (4.1)

$$\frac{1}{2}N''\delta\varphi_*^2 = \frac{3}{5}f_{\text{NL}}\zeta_1^2 \quad , \quad \frac{1}{6}N'''(\varphi_*)\,\delta\varphi^3 = \frac{9}{25}g_{\text{NL}}\zeta_1^3 \ .$$

Using this identification, we can solve the non-Gaussianity parameters in terms of the derivatives of the number of e-folds to be [70]

$$f_{\text{NL}} = \frac{5}{6}\frac{N''}{N'^2} \ , \tag{4.5}$$

$$g_{\text{NL}} = \frac{25}{54}\frac{N'''}{N'^3} \ . \tag{4.6}$$

Note that even though in order to use the ΔN-formalism one does not have to assume smallness of any initial value, the expansion of equation (4.4) converges only if $\delta\varphi_*$ is small enough. If the expansion does not converge fast enough the identification of equations (4.5) and (4.6) cannot be done.

4.2 Non-Gaussianity in Single Field Slow-roll Inflation

To compute the non-Gaussianity parameters in single field slow-roll inflation, we start out by writing the number of e-folds as

$$N = \ln\frac{a_{\text{reh}}}{a_*} \ ,$$

where a_* is the scale factor in the initial slice, and a_{reh} the scale factor in the constant density slice when ΔN is to be evaluated. By using the chain rule, we change the differentiation of N to be with respect to the moment of time when the field has its initial value,

$$N' = \frac{dt}{d\phi}\frac{dN}{dt} = -\frac{H}{\dot\phi} \ .$$

Using the chain rule again we can write

$$N'' = \frac{dt}{d\phi}\frac{dN'}{dt} = -\frac{\dot H}{\dot\phi^2} + \frac{H}{\dot\phi}\frac{\ddot\phi}{\dot\phi^2} \ .$$

Using the slow-roll approximation $3H\dot{\phi} \simeq -V'$, we can derive the intermediate results

$$\ddot{\phi} = -\frac{V''}{3H}\dot{\phi} + \frac{V'}{3H^2}\dot{H} \quad \text{and} \quad \dot{H} = \frac{1}{2\sqrt{3}}\frac{V'}{\sqrt{V}}\frac{\dot{\phi}}{M_{\text{Pl}}} \; .$$

Applying these to the expression of N'' we get

$$N'' = \frac{\sqrt{3}H}{M_{\text{Pl}}\sqrt{V}} - 3H^2\frac{V''}{V'^2} \; .$$

Remembering the definitions for the slow-roll parameters (equations 1.8 and 1.9) we can thus write

$$f_{\text{NL}} = \frac{5}{6}(2\varepsilon - \eta) \; .$$

At this order of slow-roll approximation, we can no longer neglect the intrinsic non-Gaussianity of the fields at Hubble exit, and a correction to this computation [69, 79] modifies the results so that in the squeezed limit $k_1^2 \ll k_2^2 + k_3^2$

$$f_{\text{NL}} = \frac{5}{6}(3\varepsilon - \eta) = \frac{5}{12}(1 - n_{\text{s}}) \; ,$$

where we have used the definition of the spectral index of equation (3.15). Since the observational limit for n_{s} is very strict [13], single-field inflationary models predict very small non-Gaussianity. If future experiments, e.g. the Planck mission, should detect non-Gaussianity, this would in effect rule out single-field models for inflation.

4.3 Non-Gaussianity Parameters in the Curvaton Scenario

One interesting feature of curvaton models is that they can generate significant non-Gaussianity [65, 66, 80–86]. In this section we compute the predictions for f_{NL} and g_{NL} analytically, using a formalism which is easily applicable for the simplest models.

To calculate the values of the non-Gaussianity parameters f_{NL} and g_{NL}, we first need to differentiate the number of e-folds with respect to the curvaton field initial value, σ_*. The initial moment in the definition of N is of course the end of inflation, $H = H_*$. However, the curvaton starts to oscillate when $H \simeq m$ and is very sub-dominant before that, and thus we can safely ignore the number of e-folds from the end of inflation to the beginning of oscillations, since this number is the same for all patches of the universe with different values of σ_* [70]. For generality we add a new function $\sigma_{\text{osc}}(\sigma_*)$, which is the value of the curvaton field when it starts to oscillate. For a quadratic curvaton model $\sigma_{\text{osc}}(\sigma_*) \simeq \sigma_*$.

We denote the initial time by the subscript osc, and the final time by the subscript dec. If we use the scale factors to express N, we get the expression that is to be

differentiated,

$$N = \ln \frac{a_{\text{dec}}}{a_{\text{osc}}} = \frac{1}{3} \ln \frac{\rho_{\sigma,\text{osc}}}{\rho_{\sigma,\text{dec}}} \ .$$

To calculate the derivatives, we need to differentiate both $\rho_{\sigma,\text{osc}}$ and $\rho_{\sigma,\text{dec}}$ in the logarithm. Since $\rho_{\sigma,\text{osc}} = \frac{1}{2} m^2 \sigma_{\text{osc}}^2$ this can be differentiated easily. To differentiate $\rho_{\sigma,\text{dec}}$, we first need to write

$$\left(\frac{\rho_{\sigma,\text{dec}}}{\rho_{\sigma,\text{osc}}} \right)^{\frac{1}{3}} = \left(\frac{\rho_{\text{dec}} - \rho_{\sigma,\text{dec}}}{\rho_{\text{osc}} - \rho_{\sigma,\text{osc}}} \right)^{\frac{1}{4}} \ .$$

Differentiating both sides with respect to σ_*, and then solving $\rho'_{\sigma,\text{dec}}$ yields

$$\rho'_{\sigma,\text{dec}} = \frac{8}{3} \frac{\sigma'_{\text{osc}}}{\sigma_{\text{osc}}} \rho_{\text{r,dec}} r_{\text{dec}} \ ,$$

where again

$$r_{\text{dec}} = \frac{3\rho_{\sigma,\text{dec}}}{4\rho_{\text{r,dec}} + 3\rho_{\sigma,\text{dec}}} \ .$$

Using these results, we can calculate

$$N' = \frac{2}{3} \frac{\sigma'_{\text{osc}}}{\sigma_{\text{osc}}} r_{\text{dec}} \ .$$

The first order perturbation is thus given by

$$\zeta = N' \delta \sigma_* = \frac{\sigma'_{\text{osc}}}{\sigma_{\text{osc}}} \frac{H_* r_{\text{dec}}}{3\pi} \ .$$

If $\sigma_{\text{osc}} = \sigma_*$, then this reads

$$\zeta = \frac{H_* r_{\text{dec}}}{3\pi \sigma_*} \ ,$$

which coincides with equation (3.17), as it should.

To calculate f_{NL} and g_{NL}, we need the higher derivatives of N. These quite long expressions are given by

$$N'' = \frac{2}{3} \frac{\sigma''_{\text{osc}}}{\sigma_{\text{osc}}} r_{\text{dec}} + \frac{2}{3} \left(\frac{\sigma'_{\text{osc}}}{\sigma_{\text{osc}}} \right)^2 r_{\text{dec}} \left(1 - \frac{4}{3} r_{\text{dec}} - \frac{2}{3} r_{\text{dec}}^2 \right) \tag{4.7}$$

$$\begin{aligned} N''' = {} & \frac{2}{3} \frac{\sigma'''_{\text{osc}}}{\sigma_{\text{osc}}} r_{\text{dec}} - \frac{2}{3} \frac{\sigma''_{\text{osc}} \sigma'_{\text{osc}}}{\sigma_{\text{osc}}^2} r_{\text{dec}} + \frac{2}{3} \frac{\sigma''_{\text{osc}}}{\sigma_{\text{osc}}} r'_{\text{dec}} \\ & + \frac{4}{3} r_{\text{dec}} \left(1 - \frac{4}{3} r_{\text{dec}} - \frac{2}{3} r_{\text{dec}}^2 \right) \left(\frac{\sigma''_{\text{osc}} \sigma'_{\text{osc}}}{\sigma_{\text{osc}}^2} - \frac{\sigma'^3_{\text{osc}}}{\sigma_{\text{osc}}^3} \right) \\ & + \frac{2}{3} \left(\frac{\sigma'_{\text{osc}}}{\sigma_{\text{osc}}} \right)^2 \left(r'_{\text{dec}} - \frac{8}{3} r_{\text{dec}} r'_{\text{dec}} - 2 r_{\text{dec}}^2 r'_{\text{dec}} \right) \ , \end{aligned} \tag{4.8}$$

where r'_{dec} has been calculated to be

$$r'_{\text{dec}} = \frac{2}{3}\frac{\sigma'_{\text{osc}}}{\sigma_{\text{osc}}}r_{\text{dec}}\left(3 - 2r_{\text{dec}} - r^2_{\text{dec}}\right) \ .$$

Inserting these higher derivatives into equations (4.5) and (4.6) we get [70, 84, 87]

$$f_{\text{NL}} = \frac{5}{4}\frac{1}{r_{\text{dec}}}\left(1 + \frac{\sigma''_{\text{osc}}\sigma_{\text{osc}}}{\sigma'^2_{\text{osc}}}\right) - \frac{5}{3} - \frac{5}{6}r_{\text{dec}} \tag{4.9}$$

$$g_{\text{NL}} = \frac{25}{54}\left[\frac{9}{4}\frac{1}{r^2_{\text{dec}}}\left(\frac{\sigma^2_{\text{osc}}\sigma'''_{\text{osc}}}{\sigma'^3_{\text{osc}}} + 3\frac{\sigma_{\text{osc}}\sigma''_{\text{osc}}}{\sigma'^2_{\text{osc}}}\right) - \frac{9}{r_{\text{dec}}}\left(1 + \frac{\sigma_{\text{osc}}\sigma''_{\text{osc}}}{\sigma'^2_{\text{osc}}}\right) \tag{4.10}$$
$$+ \frac{1}{2} - \frac{9}{2}\frac{\sigma_{\text{osc}}\sigma''_{\text{osc}}}{\sigma'^2_{\text{osc}}} + 10r_{\text{dec}} + 3r^2_{\text{dec}}\right] \ .$$

In the limit $\sigma_{\text{osc}} = \sigma_*$ these expressions simplify significantly, giving the predictions of non-Gaussianity for a quadratic curvaton,

$$f_{\text{NL}} = \frac{5}{4}\frac{1}{r_{\text{dec}}} - \frac{5}{3} - \frac{5}{6}r_{\text{dec}} \ , \tag{4.11}$$

$$g_{\text{NL}} = -\frac{25}{6}\frac{1}{r_{\text{dec}}} + \frac{25}{108} + \frac{125}{27}r_{\text{dec}} + \frac{25}{18}r^2_{\text{dec}} \ . \tag{4.12}$$

Since r_{dec} cannot be larger than unity, the dominant contribution to f_{NL} and g_{NL} is usually given by

$$f_{\text{NL}} \simeq \frac{5}{4}\frac{1}{r_{\text{dec}}} \quad , \quad g_{\text{NL}} \simeq -\frac{25}{6}\frac{1}{r_{\text{dec}}} \ . \tag{4.13}$$

However, if $\sigma_{\text{osc}}(\sigma_*)$ deviates from σ_* even slightly, the higher derivatives of σ_{osc} are no longer zero in the term proportional to $1/r^2_{\text{dec}}$ in g_{NL}. Even though the coefficient for this term might still be small, as r_{dec} decreases the $1/r^2_{\text{dec}}$-term starts to dominate. Thus for a curvaton with any departure from the quadratic potential we expect

$$g_{\text{NL}} \propto \frac{1}{r^2_{\text{dec}}} \propto f^2_{\text{NL}} \ . \tag{4.14}$$

The functional form of σ_{osc} encodes all dynamics of the curvaton field until it starts to undergo quadratic oscillations [84, 87], and thus the functional form of equations (4.9) and (4.10) is not really an approximation, but an exact result for an arbitrary curvaton model. It is defined as the field value at some point of time when the curvaton is oscillating in the quadratic potential, and as such, its definition is rather arbitrary. Furthermore the result for f_{NL} and g_{NL} cannot depend on the choice of σ_{osc}. Thus even though the above expressions are valid for all curvaton models, including non-quadratic, their usefulness is very limited, since in models with non-quadratic terms in their potential, all the possible non-trivial and interesting dynamics are encoded in σ_{osc} and calculating it can easily become extremely involved.

Chapter 5

Importance of Self-interactions

Until now we have considered a minimal curvaton model, described by a potential of a free massive field,

$$V(\sigma) = \frac{1}{2}m^2\sigma^2 \ .$$

However, the curvaton needs to decay, and thus it must have some interactions with other fields. Indeed, realistic models, i.e., models motivated by particle physics, have usually both interactions with other fields as well as self-interactions. These interactions can be anything from a single monomial coupling to complex polynomial interactions [88] or e.g. an axion type potential [89]. Even if the tree-level potential for the field would have no self-interactions, the necessary couplings to other fields will generate self-couplings due to loop corrections to the effective potential. Thus any curvaton model necessarily has some self-interactions.

The significance of self-interactions for the birth of the primordial perturbations is not *a priori* clear. Depending on the form of the interactions, they might not play any role at all during the evolution of the curvaton in the primordial universe. In this chapter, we will however demonstrate that even very weak self-interactions can change the evolution of the curvaton significantly. The following calculations are discussed in more detail in paper **III** for a TeV mass curvaton.

5.1   The Lower Limit for the Decay Constant Γ

In order for the initial perturbation in the curvaton field to be converted into an adiabatic curvature perturbation, the curvaton field must have interactions with the standard model degrees of freedom. The curvaton does not have to be directly coupled to these standard model degrees of freedom, as the decay may proceed via one or more

intermediate components instead. Nevertheless, we model the curvaton and its decay with a two fluid model, where the radiation fluid and the curvaton field are coupled via an interaction term in their equations of motion. The strength of this interaction is encoded in an effective coupling constant Γ. Thus the effective equations of motion for the energy densities are

$$
\begin{aligned}
\dot{\rho}_r &= -4H\rho_r + \Gamma\rho_\sigma \\
\dot{\rho}_\sigma &= -(3H + \Gamma)\rho_\sigma \ .
\end{aligned}
$$

The effective decay constant Γ here determines the moment when the curvaton decays, as the decay will occur approximately when $H \simeq \Gamma$. Thus the smaller the value of Γ, the later the curvaton decays.

The primordial perturbations have been observed to be adiabatic to a very great accuracy [90, 91]. This means that the perturbations of the energy density in all components of the primordial fluid are the same. In particular, the adiabacity of the perturbations dictates that the perturbations of the radiation and the dark matter component are the same. If the primordial perturbations are sourced by the curvaton field, this means that the curvaton must decay either to radiation before dark matter is decoupled from the radiation component, or it must decay in the right fraction to radiation and to dark matter. Since the latter scenario implies additional fine tuning, we consider the first case and what limits it imposes for the curvaton scenario. If the dark matter decouples from the primordial particle soup when $H = H_{\mathrm{DM}}$, then we need to require that the curvaton decays before that instant of time, i.e., we require $\Gamma \gtrsim H_{\mathrm{DM}}$.

Although several models of dark matter have been considered and constructed (see e.g. [92]), perhaps the most popular general idea for dark matter is a weakly interacting massive particle, or WIMP [93]. The attractiveness of a WIMP is due to what seems a happy accident, which is often referred to as the WIMP miracle: When calculating the relic abundance of a dark matter particle [94, 95], a $\mathrm{GeV} - \mathrm{TeV}$-mass particle with an annihilation cross-section typical for weak interactions produces the right amount of dark matter. A WIMP is of course not a specfic model for a dark matter particle, but rather just a generic idea or a category of theories. To investigate and predict the specific properties of the dark matter particle, one needs to specify the appropriate extension beyond the standard model.

A WIMP decouples typically at the temperature $T_{\mathrm{DM}} \sim \mathcal{O}(10)\,\mathrm{GeV}$. Since $H = \mathcal{O}(10) \times T^2/M_{\mathrm{Pl}}$, we can deduce that

$$
\Gamma \gtrsim 10^{-15}\,\mathrm{GeV} \ . \tag{5.1}
$$

It should be stressed that this lower limit for Γ is dependent on the model of dark matter; for a WIMP scenario, it might be an order of magnitude larger or smaller; for a non-thermal model of dark matter, e.g. an axion type model [96], this limit can be several orders of magnitude lower. Nevertheless, this demonstrates that the decay of the curvaton cannot occur arbitrarily late.

5.2   Bounds in the Parameter Space

To explore the importance of self-interactions, we need to find out what regions of the parameter space for the quadratic curvaton are consistent with observations, and then check for self-consistency of the quadratic assumption in those regions. There are three bounds limiting the feasibility of the quadratic curvaton model: The isocurvature bound, non-Gaussianity and the requirement that $\zeta \sim 10^{-5}$, which we call the curvature bound.

5.2.1   Curvature Bound

The most important feature of the curvaton model is its ability to produce the observed amplitude of the primordial perturbations, $\zeta \sim 10^{-5}$. According to equation (3.17),

$$\zeta = \frac{H_* r_{\text{dec}}}{3\pi \sigma_*} \ .$$

Since r_{dec} can be at most unity, we can write

$$\zeta \leq \frac{H_*}{3\pi \sigma_*} \ .$$

Solving the field value in terms of the energy density from $\rho_{\sigma *} = \frac{1}{2} m^2 \sigma_*^2$, and remembering the definition of r_*, we get

$$\zeta \leq \frac{1}{3\pi} \frac{1}{\sqrt{6 r_*}} \frac{m}{M_{\text{Pl}}} \ .$$

This can be solved to yield the curvature bound,

$$r_* \leq \frac{1}{\zeta^2} \left(\frac{m}{M_{\text{Pl}}} \right)^2 \frac{1}{54\pi} \ . \tag{5.2}$$

5.2.2   Non-Gaussianity Bound

For a quadratic curvaton the values of the non-Gaussianity parameters f_{NL} and g_{NL} are completely determined by r_{dec} according to equations (4.11) and (4.12). Since the lack of observations of non-Gaussianity limit both f_{NL} and g_{NL}, they also limit the possible values of r_{dec}. For simplicity we consider only the limits for f_{NL} and adopt the conservative limit

$$|f_{\text{NL}}| \leq 100 \ . \tag{5.3}$$

Since $r_{\text{dec}} \geq 1$, f_{NL} is dominated by the first term in the expansion of equation (4.11), so that $f_{\text{NL}} = 5/4 r_{\text{dec}}$. Substituting this into equation (5.3) results in

$$r_{\text{dec}} \geq \frac{5}{400} \ .$$

To see how the above bound translates to bounds in the (H_*, r_*)-plane, we use equation (3.17), with similar substitutions as in the previous section, to write

$$\zeta = \frac{1}{3\pi} \frac{r_{\text{dec}}}{\sqrt{6r_*}} \frac{m}{M_{\text{Pl}}} .$$

From this we can solve r_{dec} and impose the limit from the equation above,

$$r_{\text{dec}} = \frac{M_{\text{Pl}}}{m} 3\pi \sqrt{6r_*}\zeta \geq \frac{5}{400} .$$

Solving r_* from this inequality yields the non-Gaussianity bound

$$r_* \geq \frac{1}{345600\pi} \frac{1}{\zeta^2} \left(\frac{m}{M_{\text{Pl}}} \right)^2 . \tag{5.4}$$

5.2.3   The Isocurvature Bound

Since Γ is bounded from below according to the equation (5.1), this means that a certain region of the parameter space of (H_*, r_*) is also excluded: this corresponds to the region where $\zeta \sim 10^{-5}$ occurs only when Γ is too small. To see what this region is, we first relate which value of r_{dec} corresponds to a given H. To do this, we need to solve for the scale factor as a function of H.

The Friedmann equation reads

$$3H^2 M_{\text{Pl}}^2 = \rho_{\text{r}} + \rho_\sigma . \tag{5.5}$$

In the regime after the oscillations have started but before decay, the energy densities scale as

$$3H^2 M_{\text{Pl}}^2 = \rho_{\text{r}*} \frac{a_*^4}{a^4} + \rho_{\sigma*} \frac{a_{\text{osc}}^3}{a^3} .$$

Since $r_* \equiv \frac{\rho_\sigma}{\rho_{\text{r}}}\big|_*$ and $\rho_{\text{r}*} + \rho_{\sigma*} = 3H_*^2 M_{\text{Pl}}^2$, the initial densities are given by

$$\rho_{\text{r}*} = \frac{3H_*^2 M_{\text{Pl}}^2}{1 + r_*} \quad , \qquad \rho_{\sigma*} = 3H_*^2 M_{\text{Pl}}^2 \frac{r_*}{1 + r_*} .$$

Thus the Friedmann equation (5.5) can be written as

$$\frac{a^4(H)}{a_*^4} \left(\frac{H}{H_*} \right)^2 (1 + r_*) = 1 + r_* \frac{a(H)\, a^3(H = m)}{a_*^4} , \tag{5.6}$$

where we have approximated that the field starts to oscillate when $H = m$, thus $a_{\text{osc}} \simeq a(H = m)$.

To solve equation (5.6), we use the fact that $r_* \ll 1$, so we can solve the equation perturbatively. Expanding $a(H) = \sum_{n=0}^{\infty} a_n(H) \, r_*^n$, and requiring equality of both sides of the equation power by power, yields

$$\frac{a_0^4(H)}{a_*^4} \left(\frac{H}{H_*} \right)^2 = 1$$

$$4 \, a_0^3(H) \, a_1(H) \left(\frac{H}{H_*} \right)^2 + a_0^4(H) \left(\frac{H}{H_*} \right) = a_0(H) \, a_0^3(m)$$

for the zeroth and linear order in r_*. Thus

$$\frac{a(H)}{a_*} = \sqrt{\frac{H_*}{H}} \left\{ 1 + \frac{r_*}{4} \left(\frac{H_*^2}{m\sqrt{Hm}} - 1 \right) \right\} + \mathcal{O}(r_*^2) . \tag{5.7}$$

Using $\zeta = \frac{H_*}{2\pi\sigma_*} r_{\text{dec}}$, we can solve r_* to be

$$r_* = \frac{m\sqrt{m\Gamma}}{H_*^2} \frac{6 \left(\dfrac{M_{\text{Pl}}}{m} \right)^2 \zeta^2}{\dfrac{H_*^2}{m\sqrt{m\Gamma}} - 12 \left(\dfrac{M_{\text{Pl}}}{m} \right)^2 \zeta^2} . \tag{5.8}$$

If we set Γ to be its smallest possible value, we get a line in (H_*, r_*)-space, so that the parameter space to the left of it is excluded.

5.3   Importance of the Self-interactions

To discuss the importance of self-interactions for the curvaton model, one would need to specify the form of self-interactions. Indeed, myriads of different types of interactions can be listed: nearly quadratic potentials [86], monomials of different power and of different coupling constants, axion-type periodic potentials [89], washboard-type potentials [97] and others. Also other, non-scalar types of curvaton models have been considered, for example a vector curvaton scenario [98–100]. We however adopt a very simple, but arguably quite generic type of self-interaction: A monomial term suppressed by the Planck mass scale. Thus the potential reads

$$V(\sigma) = \frac{1}{2} m^2 \sigma^2 + \frac{\sigma^{n+4}}{M_{\text{Pl}}^n} . \tag{5.9}$$

Here the notation is chosen so that n measures the non-renormalizability of the self-interaction, i.e., $n = 0$ corresponds to the marginally renormalizable quartic potential.

The choice of a monomial potential is of course much simpler than a choice of a, perhaps more realistic, polynomial potential. In spite of that, typically one of the

terms of a polynomial would dominate the effect of the self-interactions, and investigating the behaviour of different values of n emulates thus also partly more generic polynomial potentials.

If the potential does not have any higher order terms, then in order for the potential to be bounded from below, n must be even. If n is not even, there must be higher even powers, which necessarily will play a crucial role in the evolution of the curvaton. Thus we limit ourselves to the cases where n is even.

The above type of self-interaction can be considered very weak: Either the interaction is of Planck scale, and thus much weaker than other known interactions, or if the suppressing mass scale is lower than the Planck scale, then the corresponding coupling constant is very small. Since a theory of quantum gravity is often presumed to produce Planck-scale corrections to effective potentials, one can also argue that the self-interaction of equation (5.9) should be present for all fields.

Note that the curvaton field might not necessarily have self-interactions at the tree level, but rather only interactions with some other degrees of freedom. As we are calculating the evolution of a classical homogeneous solution, we are interested in the effective potential where we have integrated over all quantum effects, or, as in the usual formalism, loops. These interactions will necessarily produce higher order self-interactions, and indeed, even if at the tree level the action for the curvaton would have only interactions with other fields, after integrating over those other degrees of freedom, an effective potential will surely have some self-interactions, which are typically supressed by the scale of those interactions. Since the self-interaction of equation (5.9) is suppressed by the Planck mass, these self-interactions can have an origin of very weak interactions with other fields.

If self-interactions of the forementioned type are present, then the approximation that the curvaton is purely quadratic can be safely made if and only if

$$\frac{1}{2}m^2\sigma^2 \gg \frac{\sigma^{n+4}}{M_{\text{Pl}}^n}$$

throughout the evolution of the curvaton, all the way from inflation to the decay of the curvaton. Since the energy density of the curvaton decreases monotonically as a function of time, it is sufficient to impose the above constraint only at the beginning of the evolution of the curvaton. Thus we require that

$$\frac{1}{2}m^2\sigma_*^2 \gg \frac{\sigma_*^{n+4}}{M_{\text{Pl}}^n} \ .$$

It is not *a priori* clear how much larger the quadratic term should be in order for the quadratic assumption to be a good approximation. Instead we use the limiting case when they are equal, and define σ_{eq} so that

$$\frac{1}{2}m^2\sigma_{\text{eq}}^2 = \frac{\sigma_{\text{eq}}^{n+4}}{M_{\text{Pl}}^n} \quad \Rightarrow \quad \sigma_{\text{eq}} = \left(\frac{m^2 M_{\text{Pl}}^n}{2}\right)^{\frac{1}{n+2}} . \qquad (5.10)$$

The limiting case occurs when $\sigma_* = \sigma_{\text{eq}}$, or in terms of r_*,

$$r_* = \left(\frac{m}{M_{\text{Pl}}}\right)^2 \frac{\sigma_{\text{eq}}^2}{3H_*^2}\ .$$

This defines a line in (H_*, r_*)-plane, to the right thereof the self-interactions are, at least initially, important for the evolution of the curvaton.

In figure 5.1 the parameter space is plotted with the bounds discussed in the previous section. The curvature bound and the non-Gaussianity bound are the red horizontal dashed line and the green horizontal dashed line, respectively. Thus in order for the quadratic curvaton to produce the observed amplitude of primordial perturbations with not too large non-Gaussianity, the initial conditions should between those two dashed lines. The isocurvature bound is the blue curve drawn with a dash dot line, and thus in order for the quadratic curvature not to produce isocurvature, assuming a WIMP-type dark matter, the initial conditions should lie right of that line. Finally, the black solid line is the line where the quadratic and the non-quadratic terms in the potential are initially equal. Thus in order for the quadratic assumption to be a good approximation, the initial conditions should lie left of that black line. Thus the allowed quadratic regime is the trapezoid limited by all the different lines so that the black line is the right edge of the trapezoid.

In general, one can draw the conclusion that the lower the value of n is, the less allowed quadratic regime there is. For $n = 4$ there is quadratic regime left for both plotted values of mass, where as for $n = 0$ no quadratic regime is left for these choices of m. Additionally the increase in the magnitude of the mass has a general trend of creating more allowed quadratic regime.

For $n = 0$, which corresponds to the quartic self-coupling, there is no quadratic regime left, even for the higher mass, $m = 10^8\,\text{GeV}$. This is perhaps not too surprising, since the interaction is no longer weak, but actually strongly coupled. This can be seen by looking at the choice of the self-interaction (equation (5.9)) for $n = 0$: While for higher values of n the powers of Planck mass in the denominator guarantee that the interaction is indeed weak, for $n = 0$ there are no powers of Planck mass in the denominator, and the effective coupling constant is unity. If one would add a weak coupling constant to the quartic self-coupling, the line of equality for the mass term and for the self-coupling (the black solid line) would move to the right and for a small enough coupling there would be allowed quadratic region in the parameter space.

For $n = 2$ there is no allowed quadratic region left for the mass of $10^4\,\text{GeV}$, where as for the higher value of the mass, $m = 10^8\,\text{GeV}$ there is still some quadratic region left. For $n = 4$ for both choices of mass there is some allowed quadratic region, though for the smaller value of the mass the region is very small.

As a conclusion the effect of self-interactions can be said to be very important: For some choices of n and m there is some region in the parameter space where the quadratic approximation is consistent, even though there a large region where the self-interactions become important. For other choices of n and m there is no area in

the parameter space where the quadratic approximation would be a good one. Thus the investigation of the effects of self-interactions to the evolution of the curvaton is well motivated for all choices of parameters, and absolutely crucial to understand the predictions of the curvaton model.
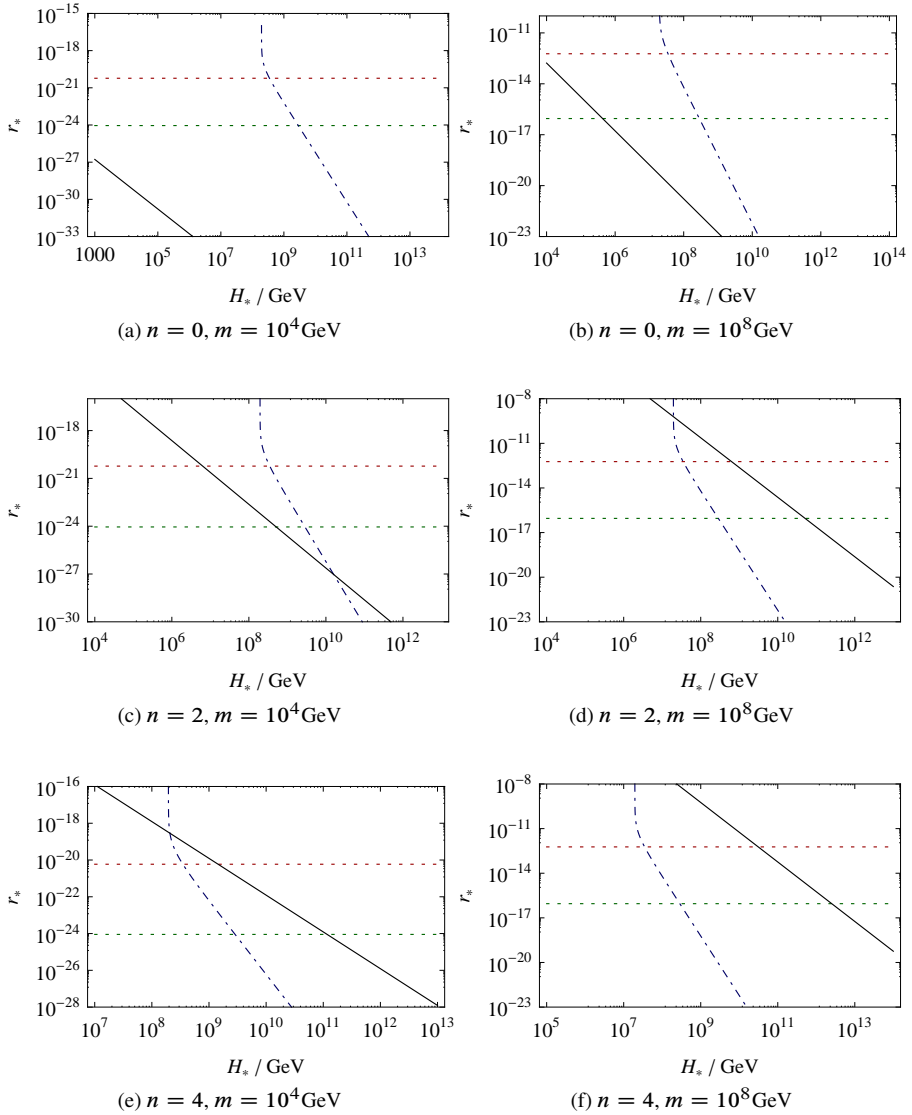
Figure 5.1: The parameter space and different bounds for quadratic curvaton models. The red dashed line is the curvature bound (section 5.2.1), the green dashed line is the bound arising from limits on non-Gaussianity (section 5.2.2), and the blue dash-dotted line is the isocurvature limit (section 5.2.3). Thus the allowed region for the curvaton is the area right from the blue dash-dotted line, and between the red and green dashed lines. The black curve signifies the initial equality of the quadratic and non-quadratic terms in the potential, thus the self-interactions become significant right of the black solid line.

Chapter 6

Dynamics of Self-interactions

In the previous chapter we introduced self-interactions for the curvaton. We also demonstrated that for some choice of m and n, these self-interactions are relevant in significant regions of the parameter space, whereas for some other choice of m and n they are relevant everywhere in the parameter space. There the initial field value is such that the non-quadratic self-interaction initially dominates the mass term in the potential, $\sigma_* > \sigma_{eq}$.

The self-interaction is relevant when the field value, or the amplitude of its oscillations, is high enough to reside in the non-quadratic part of the potential. It turns out that the non-quadratic form of the potential modifies the scaling solution of an oscillating field in such a significant way that the predictions of the curvaton model become non-linear and highly dependent on the initial conditions. The analysis in this chapter is based on the more detailed discussion in papers **I** and **II**.

6.1   Analytical Estimates for the Self-interacting Case

In general adding a new monomial term to the potential of the curvaton modifies its evolution in time. Assuming that one term in the potential dominates at a time, we can divide the evolution of the curvaton roughly into four separate phases:

1. After inflation ends, the curvaton is still in slow-roll, $H^2 \gg V''(\sigma_*)$, and the field value stays fixed, $\sigma = \sigma_*$.

2. As H decreases sufficiently, the field becomes massive compared to the Hubble friction term in its equation of motion, $H^2 \sim V'(\sigma_*)$, and the field starts to move more rapidly towards its minimum. If $n \geq 6$ the field merely rolls slowly down until it reaches the quadratic regime [53], but for $n \leq 4$ the field undergoes oscillations around its minimum. Given that $\sigma_* > \sigma_{eq}$, these oscillations are affected by the non-quadratic term of the potential.

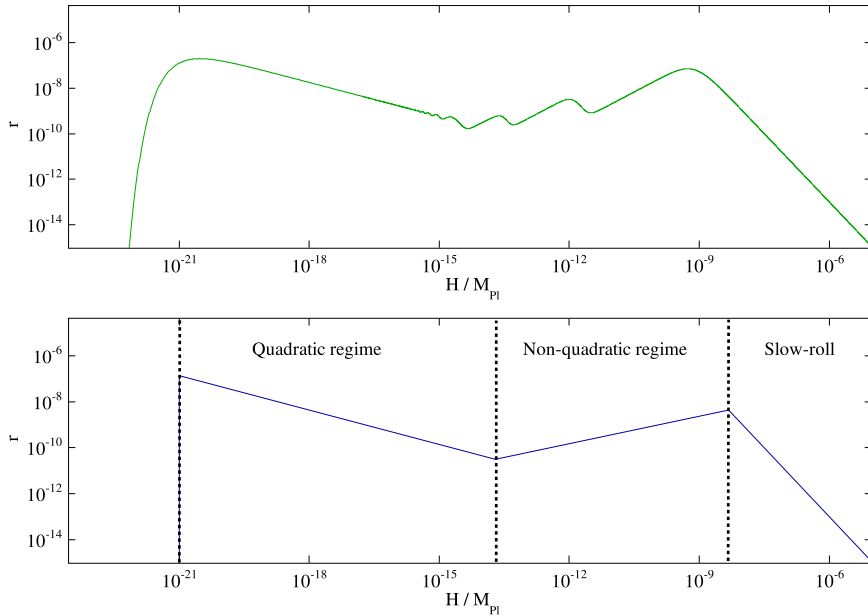Figure 6.1: Comparison between the numerical solution and and analytical approxi-mations. $n = 4$, $m = 10^4\,\text{GeV}$, $H_* = 10^{13}\,\text{GeV}$, $\Gamma = 10^{-3}\,\text{GeV}$, $r_* = 10^{-15}$. The horizontal axis is H in units of M_{Pl}. As H decreases with time, time runs from right to left in this plot. Note that in order for $\zeta \sim 10^{-5}$, the value of Γ should be adjusted to be significantly smaller.

3. As the universe expands, the amplitude of the oscillations of the curvaton de-creases, and slowly the importance of the non-quadratic term starts to diminish. Once $\sigma \sim \sigma_{\text{eq}}$, the field oscillations become almost purely quadratic, so that the energy density of the field scales as $\rho_\sigma \propto a^{-3}$.

4. Once the Hubble constant has decreased such that $H \sim \Gamma$, the curvaton decays into radiation, transforming the initial mixed perturbation into an adiabatic per-turbation.

As stated above, if n is sufficiently large, the evolution of the field in the non-quadratic part of the potential is not oscillatory, but rather merely decaying. For sim-plicity, and due to the fact that the cases $n \geq 6$ evolve smoothly and thus produces no unexpected results, for the rest of this work we consider mostly the cases $n \leq 4$, which have non-linear oscillatory behaviour.

In the stages 1, 3 and 4 of the curvaton evolution, there is a clear approxima-tive solution. However, for the period of non-quadratic oscillations there is no valid analytical solution. In section 3.2 we derived a scaling law solution for the energy

density of the curvaton when it is oscillating rapidly in a monomial potential. If the field would be oscillating extremely fast compared to the background evolution, and the amplitude of the oscillation would be very large, so that the non-quadratic term would dominate the quadratic term for most of the oscillation, then this approximation would be valid. These different phases and their approximations are demonstrated in figure 6.1. It illustrates clearly that while the oscillations in the quadratic regime are fast enough for the scaling solution to be a good approximation, for the non-quadratic regime the situation is not as evident.

Since the evolution of the self-interacting curvaton follows that of the quadratic curvaton once the amplitude of the oscillations has decreased sufficiently, in principle the notation of section 4.3 is still valid. Thus the equations for ζ, f_{NL} and g_{NL} look deceivingly similar to the quadratic case. Even so, the non-linearity of the self-interacting model is merely hidden in the function $\sigma_{\mathrm{osc}}(\sigma_*)$, which evolves in a non-trivial, and as we shall see later on, oscillatory manner.

The approximative analysis stated above applies only for the homogeneous background field value of the curvaton. For the quadratic model the homogeneous field value and the perturbation had the same (linear) equation of motion, so that the relative perturbation stayed constant. In the non-quadratic case, the equation of motion for the perturbation is very different,

$$\ddot{\delta\sigma} + 3H\dot{\delta\sigma} + V''(\sigma)\,\delta\sigma = 0 \ .$$

Now the evolution of the perturbations depends in a non-linear way on the evolution of the background solution. Thus it is no longer sufficient to solve for the field value when it decays, but rather we need to solve both the background EOM as well as the EOM for the perturbation. In practice it is usually simpler to use the ΔN-formalism, so that one does not need to solve the EOM for the perturbation separately, but rather it is sufficient to solve the background equation multiple times.

6.2   Numerical Analysis

In the previous section we discussed analytical approximations for the self-interacting curvaton scenario, in a similar fashion to what we did for the quadratic case in the previous chapter. Be that as it may, due to the non-linearity of the self-interacting model we need to resort to numerical methods to take into account the evolution in the non-quadratic part of the potential. Since we are solving the model numerically, we can also dispose of the other approximations we have made, most important of those being the instantaneous decay.

To compute the predictions of the self-interacting curvaton model of equation (5.9) numerically, we use the ΔN-formalism to compute the primordial perturbation amplitude and the corresponding non-Gaussianity parameters. The system of

equations that we need to solve is given by

$$\ddot{\sigma} + (3H + \Gamma)\dot{\sigma} + m^2\sigma + (n+4)\frac{\sigma^{n+3}}{M_{\mathrm{Pl}}^n} = 0,$$

$$\dot{\rho}_{\mathrm{r}} = -4\rho_{\mathrm{r}} + \Gamma\dot{\sigma}^2 \qquad (6.1)$$

$$3H^2 M_{\mathrm{Pl}}^2 = \rho_{\mathrm{r}} + \rho_{\sigma}.$$

Also, the initial conditions are specified by the previously introduced two free parameters, H_* and r_*, so that the initial energy densities are given by

$$\rho_{\mathrm{r}} = 3H_*^2 M_{\mathrm{Pl}}^2,$$

$$\rho_{\sigma} = V(\sigma_*) = r_*\rho_{\mathrm{r}}.$$

The initial velocity of the curvaton field is assumed to be negligible, $\dot{\sigma}_* = 0$.

Since when using the ΔN-formalism we are investigating differences in evolution of two separate patches, we need to specify different initial conditions for the patches. In the other patch the initial conditions are given by the background, while the other one has otherwise similar initial conditions, but the initial curvaton field value has a small perturbation, originating from the quantum fluctuations described in section 3.1,

$$\sigma_1 = \sigma_* \quad , \quad \sigma_2 = \sigma_* + \frac{H_*}{2\pi}.$$

The final amplitude of the primordial perturbation is then given by evolving the system until the curvaton has decayed, and then comparing the number of e-folds in the two different patches at a fixed value of H. In principle the full system, described by the system of equations (6.1), should be used all the way until this final constant energy density slice. Having said that, solving this set of differential equations is very slow at the end of the simulation: As the field enters the quadratic regime, the oscillations become extremely rapid. Since several steps are needed for each cycle of oscillation, the solution becomes increasingly slow to compute deep in the quadratic regime. To circumvent this, we use the fact that when the field is oscillating in a quadratic potential, in the limit of fast oscillations it satisfies a relation $\langle\frac{1}{2}\dot{\sigma}^2\rangle = \langle\frac{1}{2}m^2\sigma^2\rangle$, analogous to a harmonic oscillator. This means that in the limit of infintely fast oscillations in the quadratic regime, the system has one degree of freedom less, and the behaviour of the curvaton field can be described perfectly by a single degree of freedom, here chosen to be the energy density, ρ_{σ}. This energy density has then a well-behaving scaling law, $\rho_{\sigma} \propto a^{-3}$. Thus after the quadratic term dominates sufficiently, $\frac{1}{2}m^2\sigma^2 \gg \frac{\sigma^{n+4}}{M_{\mathrm{Pl}}^n}$, we can safely switch to solving an approximate system, described by the equations

$$\dot{\rho}_{\sigma} = -(3H + \Gamma)\rho_{\sigma},$$

$$\dot{\rho}_{\mathrm{r}} = -4\rho_{\mathrm{r}} + \Gamma\rho_{\sigma}, \qquad (6.2)$$

$$3H^2 M_{\mathrm{Pl}}^2 = \rho_{\mathrm{r}} + \rho_{\sigma}.$$

This corresponds to the approximation that the field is oscillating in a purely quadratic potential very fast compared to the background solution. We have checked the numerical stability, and confirmed that the error created by this approximation is diminishingly small.

After the curvaton has decayed, we then calculate the difference of number of *e*-folds in the two patches. This must be done in a uniform-density slicing, i.e., the two patches must be evolved to the same value of H. The difference in N in the two patches is then directly ζ.

6.2.1 Non-Gaussianity

To compute the non-Gaussianity parameters in the ΔN-formalism, we use equations (4.5) and (4.6) where f_{NL} and g_{NL} are expressed as fractions of derivatives of the total number of *e*-folds with respect to the initial field value σ_*. Since numerical methods have finite accuracy, the derivatives are calculated as finite differences. This is done using a numerical method called *five-point stencil* [52]. In this method, the derivatives of a function $f(x)$ are expressed as linear combinations of values of $f(x)$, different number of h-sized steps away from x. For f_{NL} and g_{NL} we need the three first derivatives, and these are given by the expressions

$$
\begin{aligned}
f'(x) &= \frac{-f(x+2h) + 8f(x+h) - 8f(x-h) + f(x-2h)}{12h} \,, \\
f''(x) &= \frac{-f(x+2h) + 16f(x+h) - 30f(x) + 16f(x-h) - f(x-2h)}{12h^2} \,, \\
f'''(x) &= \frac{f(x+2h) - 2f(x+h) + 2f(x-h) - f(x-2h)}{2h^3} \,.
\end{aligned}
$$

The five-point stencil has the advantage compared to many other finite difference methods that the error made using these formulae is of order $\mathcal{O}(h^4)$.

For the calculation of the derivatives of N, we calculate the above expressions with different values of the finite interval h, which is then adjusted dynamically to minimize the contribution of numerical noise and inaccuracy arising from the finiteness of h.

6.3 Evolution of r

To gain some insight into the evolution of the self-interacting curvaton, it is often more practical to follow the evolution of the energy fraction in the curvaton, defined by

$$
r \equiv \frac{\rho_\sigma}{\rho_\sigma + \rho_{\mathrm{r}}} \,,
$$

than the evolution of the field value $\sigma(t)$. Indeed, since we solve the approximate system of equation (6.2) once we enter the quadratic regime, the field value is not always uniquely determined by the program.
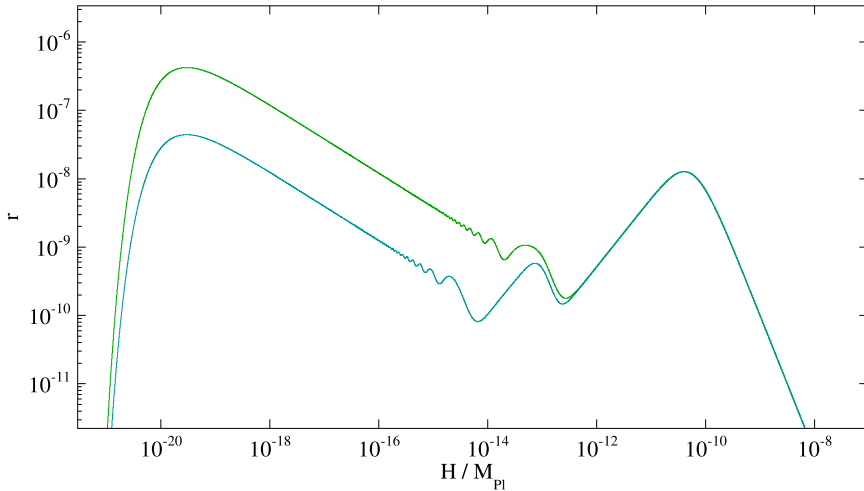
Figure 6.2: The evolution of the energy fraction r in time. $H_* = 10^{-7} M_{\rm Pl}$, $\Gamma = 10^{-2}$ GeV, $n = 4$ and $r_* = 10^{-14}$. The lower curve has the mass $m = 10^4$ GeV, whereas the upper curve has the mass $m = 10^5$ GeV. Note that for better visibility Γ has been set far too small to get $\zeta \sim 10^{-5}$.

As expected and already briefly discussed in section 6.1, the curvaton is initially in slow-roll and evolves slowly. Since σ stays roughly constant, but the background radiation component dilutes as $\propto a^{-4}$, r increases. After H has decreased sufficiently, the field, as well as the energy fraction r, starts to oscillate. As the field is still in the non-quadratic part of the potential, the energy density of the curvaton scales down approximately as calculated in section 3.2, that is, for $n > 0$ it dilutes faster than that of the background radiation, and thus r decreases. Note that since the oscillations occur now in the non-quadratic regime, ρ_σ does not scale down smoothly, but with an oscillatory envelope. After r and the field value of the curvaton have scaled down sufficiently, the contribution of the non-quadratic term to the potential becomes negligible, and the field starts to undergo almost purely quadratic oscillations. In the quadratic regime the equality $\langle \frac{1}{2}\dot{\sigma}^2 \rangle \simeq \langle \frac{1}{2}m^2\sigma^2 \rangle \simeq \langle V(\phi) \rangle$ holds and the evolution of r becomes smooth.

If the oscillations in the non-quadratic part of the potential would have a similar (short) period as the oscillations in the quadratic regime, the value of r would depend smoothly on the initial conditions. However, the periods differ by several orders of magnitude. This causes the phase of the oscillation in the non-quadratic regime to be frozen in when the oscillations change abruptly to quadratic oscillations. This is demonstrated in figure 6.2. Here the curvaton is evolved with otherwise similar parameters and initial conditions, but in the upper green line the mass has been cho-

sen to be 10^5 GeV, where as in the lower blue one it has been chosen to be 10^4 GeV. Since the mass determines when the transition from the non-quadratic to the quadratic regime occurs, the decrease of mass delays the transition a bit. However, as the oscillations in the non-quadratic regime are quite slow, the transitions happen in completely different phases of the oscillations: one at the top of an oscillation, while the other at the bottom of an oscillation. Since the initial conditions for the quadratic oscillations thus differ significantly, so do their later evolution: The curvaton which switched to the quadratic regime on the top of an oscillation has much larger value of r later on than the curvaton which initiated its quadratic oscillations on the bottom of an oscillation.

Note that in order for this effect to be significant, the regime of transition, that is, the regime where both the quadratic and the non-quadratic term in the potential are significant, must be shorter than the period of an oscillation in the non-quadratic regime. Otherwise the initial value for the quadratic oscillations would be an average over several oscillations in the non-quadratic regime.

6.4   Evolution of ΔN

Although the non-quadratic oscillations can be slow when compared to the background dynamics, the oscillations are nevertheless smooth: The evolution of r in figure 6.2 look quite close to a power law multiplied by some sinusoidal oscillation. However, we are not interested in the value of r, but rather the amplitude of the primordial perturbations and the value of the non-Gaussianity parameters. In figure 6.3 we have plotted the evolution of ΔN for a given set of parameters as a function of H. Although the evolution of r is smooth, ΔN demonstrates very non-trivial behaviour.

There are several qualitative features manifest in figure 6.3. Firstly, the general envelope of the curve, averaged over the oscillations, follows approximately that of r. This merely reflects equation (3.16), which states that the total perturbation, here given by ΔN, is the perturbation in σ multiplied by the efficiency factor, which is roughly given by r. Thus the evolution of the general amplitude of ΔN, discarding the oscillatory features, is explained by the changes in the energy fraction in the curvaton: ΔN decreases in the non-quadratic regime as r decreases, and ΔN increases as the curvaton starts to undergo quadratic oscillations and r starts to increase. Moreover, when the curvaton decays, the mixed perturbation in the curvaton is transformed into the adiabatic perturbation of the total fluid, and thus ΔN freezes to its constant value.

The oscillations of ΔN are however more difficult to understand. The oscillations in the non-quadratic regime appear very non-sinusoidal, as the full oscillation cycle consists of two very different half-cycles. Again, since the evolution is very smooth in the quadratic regime, the value that ΔN has during the transition from the non-quadratic to the quadratic regime freezes in as the initial value for the quadratic evolution. Thus the final value of ΔN is very sensitive to the phase of the non-quadratic oscillations when the transition occurs.
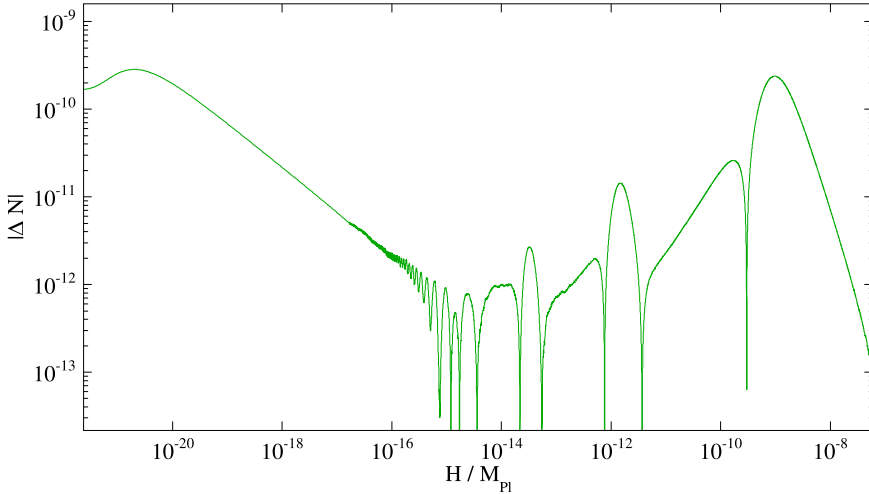
Figure 6.3: Plot of the evolution of ΔN as a function of H. $H_* = 10^{13}$ GeV, $m = 10^4$ GeV, $\Gamma = 10^{-3}$ GeV, $n = 4$, and $r_* = 10^{-15}$. Note that in order for $\zeta \sim 10^{-5}$, the value of Γ should be adjusted to be significantly larger.

Also noteworthy is the fact that though we actually plot $|\Delta N|$ due to the logarithmic plot, the sign of ΔN actually oscillates: In the oscillations in the non-quadratic regime every other half-cycle of the oscillations has an opposite sign from its neighbouring half-cycles. Thus if the switch to the quadratic regime would occur during a half-cycle with a negative sign, the final value of the perturbation would have an opposite sign to that of the initial perturbation. While this feature has no definite observational signature, it demonstrates the very counter-intuitive dynamics present: The patch which had initially *higher* energy density than the average, can have *lower* energy density in the final slice, and vice versa.

6.5   Oscillations in the Parameter Space

As demonstrated in the previous sections the long period of oscillations in the non-quadratic regime causes the phase of the non-quadratic oscillation to freeze in, so that its value during the transition from the non-quadratic to the quadratic regime affects the final values of r and ΔN significantly. Thus any small change of parameters which affect either the phase of the non-quadratic oscillations or the point of transition from the quadratic to the non-quadratic regime can change the final values by a large amount.

Almost all of the parameters and initial conditions can affect the point of transition and the phase of the non-quadratic oscillations: Since m determines the value of σ_{eq}, it
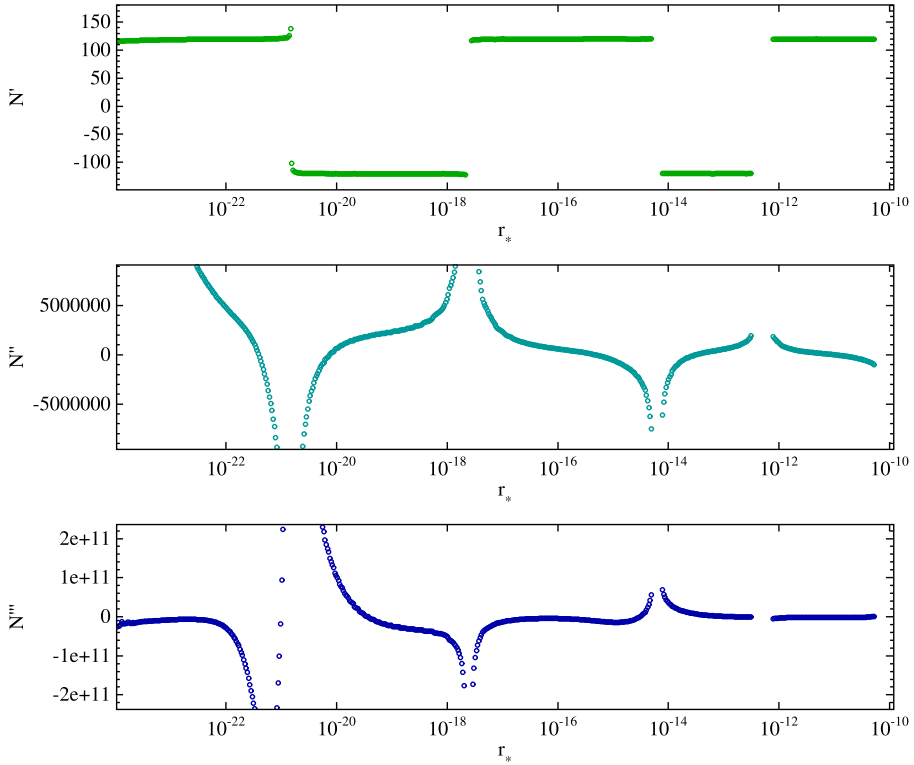
Figure 6.4: N', N'' and N''' plotted against r_*. The other parameters are given by $n = 4$, $m = 10^6\,\text{GeV}$, and $H_* = 10^{12}\,\text{GeV}$. The missing intervals in the plots correspond to those combinations of parameters which cannot produce $\zeta \sim 10^{-5}$.

also determines what is the value of H when the transition from the non-quadratic to the quadratic regime occurs. r_* plays the role of determining the initial homogeneous value of the field, σ_*. The initial amplitude of the perturbation is determined by H_*. Different values of n corresponds to different behaviours in the non-quadratic regime. Thus if we would plot ΔN or its derivatives as a function of any of the forementioned parameters, we would see oscillatory behaviour.

In figure 6.4 we have plotted the values of N', N'' and N''' as a function of r_* for fixed values of H_*, m and n. Here the value of N' can be seen to have a nearly fixed magnitude. This can be understood by N' approximately determining the amplitude of the perturbation through the formula $\zeta \simeq N'\delta\sigma_*$. Since H_* is fixed, so is $\delta\sigma_*$, and in order to get $\zeta \sim 10^{-5}$, N' must also have almost a fixed value. This is realized by tuning the value of Γ appropriately. N' nevertheless can change sign, and since $\delta\sigma_*$ is fixed, also ζ can change sign. Again, the sign of the primordial perturbation is not
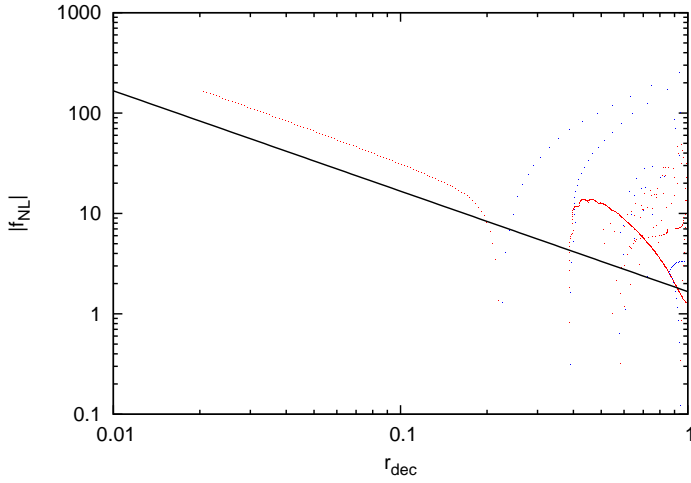
(a) $|f_{NL}|$ plotted against r_{dec} for a fixed value of $H_* = 5 \times 10^{12}$ GeV. Red points coresponds to $f_{NL} > 0$ and blue points to $f_{NL} < 0$.
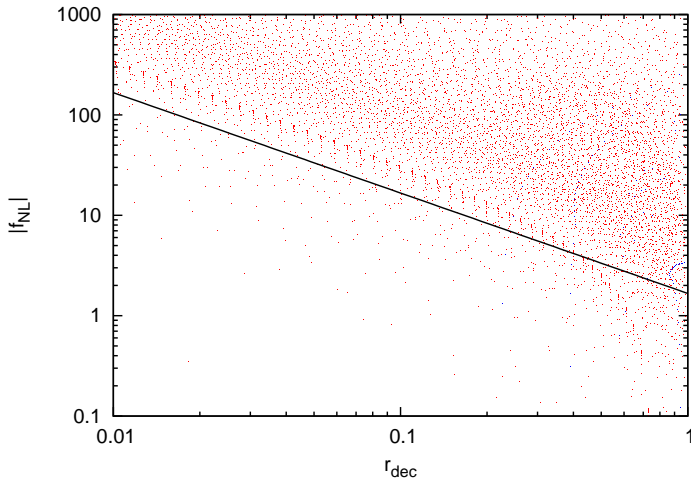
(b) $|f_{NL}|$ plotted against r_{dec} for all values of H_* and r_*.

Figure 6.5: The behaviour of $|f_{NL}|$ for a self-interacting curvaton model with $n = 4$ and $m = 10^6$ GeV. Only those points are plotted which produce the correct amplitude for the perturbations in the range $H_* = 10^9 \ldots 10^{13}$ GeV and $r_* = 10^{-24} \ldots 10^{-8}$.

observationally significant, but it does result in the counterintuitive result that patches that were overdense in the very early universe become *under*dense later on.
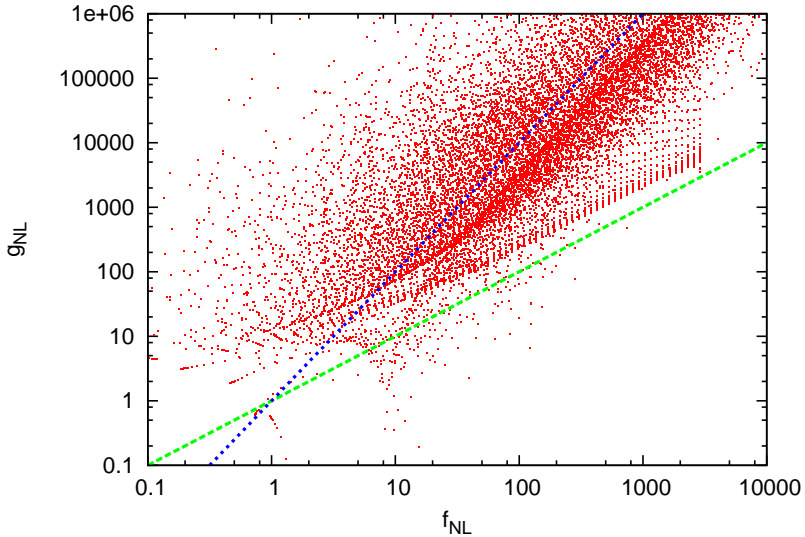
Figure 6.6: $|g_{\mathrm{NL}}|$ plotted against $|f_{\mathrm{NL}}|$ for all values of H_* and r_* which produce the correct amplitude for the perturbations in the range $H_* = 10^9 \ldots 10^{13}$ GeV and $r_* = 10^{-24} \ldots 10^{-8}$. The green line corresponds to the linear relation $g_{\mathrm{NL}} \sim f_{\mathrm{NL}}$ and the blue lines to the quadratic relation $g_{\mathrm{NL}} \sim f_{\mathrm{NL}}^2$. Other parameters are given by $n = 4$ and $m = 10^6$ GeV.

Even though Γ is adjusted so that N' does not oscillate, the same does not apply for the higher derivatives: Both N'' and N''' oscillate wildly, also changing signs. This is a direct consequence of the slow non-quadratic oscillations. As r_* is changed, the number of oscillations that the curvaton undergoes before the transition to the quadratic regime changes, and the phase of the non-quadratic oscillation freezes in producing the observed oscillations of the derivatives of N as a function of the initial conditions.

6.6 Comparison with the Analytical Estimates for f_{NL} and g_{NL}

To demonstrate the non-linear and oscillatory behaviour of the self-interacting curvaton, we compare the numerical results with the analytical expression calculated for f_{NL} and g_{NL}. In figure 6.5(a) the value of $|f_{\mathrm{NL}}|$ is plotted against r_{dec} for a fixed value of H_* and r_* between 10^{-24} and 10^{-8} for $m = 10^6$ GeV and $n = 4$. In the figure we can see the analytical estimate of equation (4.13) drawn as the black line, whereas

the red dots corresponds to the numerical results. From that we can see that while the analytical expression for f_{NL} roughly applies, the oscillations can signifcantly change the value of f_{NL}.

In figure 6.5(b) we have plotted all allowed points in the parameter space for a model with $m = 10^6$ Gev and $n = 4$. As we allow H_* to take different values, a family of curves is drawn, where each curve is similar to the curve present in figure 6.5(a), but each with a bit different oscillatory features, resulting into the noisy scatter present in the plot. Again we can see that the analytical result functions as an attractor, though most of the points are scattered aobve the line.

In figure 6.6 the value of $|g_{NL}|$ is plotted against the value of $|f_{NL}|$. The green line corresponds to the analytical expression for the quadratic curvaton in equation (4.13), and the blue line correponds to an analytical estimate for a non-quadratic curvaton in equation (4.14). We can see that there is a wide accumulation of points near the green line, which corresponds to that area of the parameter space which is already initially in the quadratic regime. Similarly there appears to be a build-up of points near the blue line. In spite of that, most of the points are scattered around the plot.

Most points give rise to a larger f_{NL} than one would expect from the analytical $1/r_{dec}$-estimate, however since f_{NL} can actually change sign, points can always be found where f_{NL} is arbitrarily close to zero. It is also interesting to note that several different values of f_{NL} correspond to a given point r_{dec}, since different choices of initial conditions can be degenerate yielding the same r_{dec}. It is also noteworthy that for a given fixed value of r_{dec}, there are multiple sets of parameters which all give rise to the same final amplitude for the perturbations but different value of f_{NL} and g_{NL}.

Chapter 7

Results in the Parameter Space

The numerical method described in the previous chapter can compute the amplitude of the primordial perturbations, ζ, produced by a self-interacting curvaton for a set of parameters $\{n, m, H_*, r_*, \Gamma\}$. To find out what combinations of the parameters can produce perurbations compatible with observations, we first fix n and m, and then scan through the parameter space spanned by H_* and r_*. We then impose constraints to ensure that we are left with only those points in the parameter space which are compatible with observations. The complete scan of the parameter space is performed in paper **I** and **II**, with the latter paper focusing on the non-Gaussianities created by the self-interacting curvaton.

7.1 Allowed Regions of the Parameter Space

To make sure that the amplitude of the perturbations is correct we adjust the value of the effective decay constant Γ at each point in the (H_*, r_*)-space so that $\zeta \sim 10^{-5}$. Since decreasing Γ postpones the decay and thus makes the curvaton more dominant, smaller Γ translates to larger ζ. However, when the curvaton is already completely dominant when it decays, $r_{\mathrm{dec}} \sim 1$, decreasing Γ has no effect. Thus if $\zeta < 10^{-5}$ even when $r_{\mathrm{dec}} \simeq 1$, then that point in the parameter space cannot produce the observed perturbations and thus that combination of the parameters is ruled out.

Note that the choice of which parameter to adjust while keeping the other parameters fixed is not unique. Instead of adjusting Γ, we might just as well adjust r_* to try achieve the correct amplitude for ζ. Be that as it may, adjusting Γ is often easier, since the amplitude of ζ increases monotonously as a function of Γ, but not as a function of r_* etc.

As discussed in section 5.1, the curvaton must produce only adiabatic modes when

it decays, and thus it must decay before dark matter decouples. By assuming that the DM particle is a generic WIMP, we get a lower limit for Γ (see section 5.1), which depends on the DM decoupling temperature. In papers **I** and **II**, we adopted the limit $\Gamma > 10^{-15}$GeV, corresponding to a decoupling temperature $T_{\mathrm{DM}} \sim \mathcal{O}(\mathrm{GeV})$, and in paper **III** the more conservative limit $\Gamma > 10^{-17}$GeV. Note that the choice of the lower limit is somewhat arbitrary, since it depends on the details of the DM model. We then discard those points in the parameter space which would require too small Γ to produce $\zeta \sim 10^{-5}$.

The curvaton can potentially produce non-Gaussianity so large that it would be in conflict with current observations, and thus those areas of the parameter space must be discarded. The current best observational limits are given in equations (4.2) and (4.3) [31, 76]. We thus compute the values of f_{NL} and g_{NL} for each point left in the parameter space, and discard those which produce non-Gaussianity incompatible with the limits mentioned above.

The amount of tensor perturbations in the early universe is determined by the inflationary scale H_*, and is not dependent on the field value of the inflaton. Thus observations of the tensor modes would be a direct observation of the inflationary scale. The observational limit for the tensor modes is usually given by the tensor-to-scalar ratio defined by

$$r \equiv \frac{\mathcal{P}_{\mathrm{g}}(k)}{\mathcal{P}_{\mathcal{R}}(k)} \ ,$$

where $\mathcal{P}_{\mathrm{g}}$ is the power spectrum for the tensor modes defined analogously with section 2.4. The current best bounds for r are given by $r < 0.36$ from the CMB alone, or $r < 0.20$ where the CMB data is combined with data from baryonic acoustic oscillations and supernovae observations [13]. The stricter value translates to a limit for the inflationary scale

$$H_* < 2.99 \times 10^{14} \mathrm{GeV} \ .$$

To sum up, each point in the parameter space is evaluated with the following criteria:

1. There must be a value of Γ such that $\zeta \sim 10^{-5}$.

2. That value of Γ cannot be smaller than the limit given by the isocurvature bound.

3. The non-Gaussianity parameters must be within observational limits, $-9 < f_{\mathrm{NL}} < 111$ and $-3.5 \times 10^5 < g_{\mathrm{NL}} < 8.2 \times 10^5$.

4. The inflationary scale cannot be too large, as constrained by the tensor-to-scalar ratio.

If the point in the parameter space passes all these tests, then we conclude that a curvaton model with that set of parameters could be responsible for the primordial perturbations that we observe.
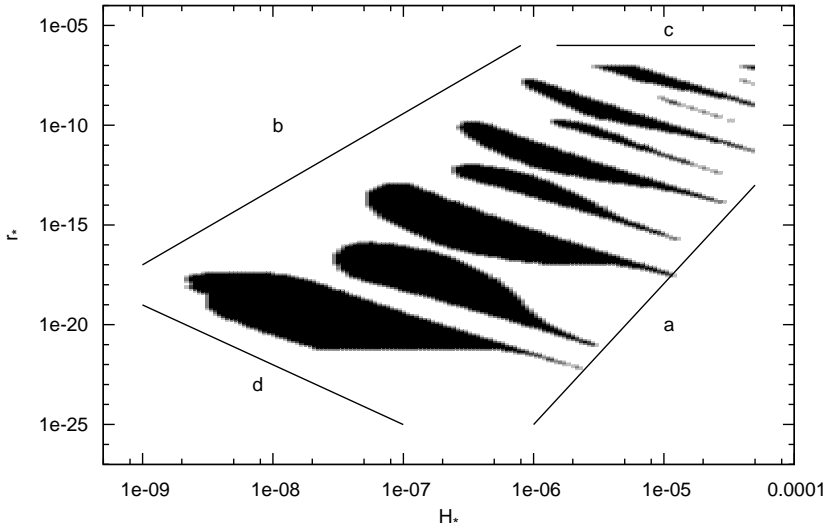
Figure 7.1: A schematic plot of the effect of different constraints in the parameter space. Line *a* is the bound imposed by limits on non-Gaussianity, line *b* demonstrates the limit originating from the initial perturbation being smaller than 10^{-5}, line *c* is the requirement that the curvaton needs to be massless and very subdominant during inflation, and line *d* is the isocurvature limit.

7.2 Effect of Constraints in Parameter Space

The different bounds originating from different observational limits mentioned in the previous section make cuts in different regions of the parameter space. To illustrate these different constraints and their effect in the allowed region of the parameter space, we have plotted their effect schematically in figure 7.1.

The line *a* indicates the cut made by the observational limits for f_{NL} and g_{NL}. In the part of the parameter space dominated by the non-quadratic part of the potential, r_{dec} increases from lower right to the upper left corner. Without the oscillations the non-Gaussianity parameters would be given by roughly $f_{\mathrm{NL}} \propto 1/r_{\mathrm{dec}}$ and $g_{\mathrm{NL}} \propto 1/r_{\mathrm{dec}}^{2}$, and thus the cuts produced by these constraints would be direct lines in the direction indicated by line *a*. However, due to the oscillations in the parameter space, both f_{NL} and g_{NL} increase un-monotonically as a function of r_{dec} and thus the cut produced by constraints is not a straight line. Nevertheless, the parameter space

in the region indicated by the line a is mostly limited by non-Gaussianity.

The cut indicated by line b is due to the initial perturbations in the curvaton field being too small to evolve into the final perturbation of 10^{-5}. If the homogeneous curvaton field value and its perturbation would obey the same equation of motion, the relative perturbation would stay fixed all the way until decay, and then the amplitude of the perturbation would be given by

$$\zeta \simeq r_{\text{dec}} \frac{H_*}{3\pi\sigma_*} \ .$$

The efficiency factor is given by $r_{\text{dec}} \leq 1$, and thus if the initial perturbation given by $H_*/2\pi\sigma_*$ is smaller than the required ζ, then the curvaton cannot produce the observed perturbations under any conditions. This limit would be given by a straight line such as the line b. However, the curvaton field value and its perturbation have different equations of motion, and thus the final value of the relative perturbation is not completely determined by the initial value, but instead is affected by the non-linear dynamics. Thus the cut is not given by a straight line, but rather by an oscillatory curve.

The upper region of the parameter space is limited by several factors, indicated by line c. The higher the value of r_*, the more massive the curvaton is during inflation. If the curvaton is too massive, it is no longer in slow-roll, but rather the value of the field can change significantly during inflation. This would lead to a running of the spectral index, and thus we require that the curvaton is effectively massless during inflation, $V'' \ll H_*^2$. Note that since also the running of the inflaton and thus H_* will also produce running of the spectral index, we have not quantified this limit explicitly, as the exact limit will depend on the details of the inflationary model [101]. It might even be possible to produce a model where with some fine-tuning the curvaton and the inflaton would evolve appropriately to produce a scale invariant spectrum even though neither the inflaton nor the curvaton would be in slow-roll. Additionally the limit indicated by line c also ensures that the perturbative treatment that we have used is applicable: We have assumed that the curvaton is completely subdominant during inflation and thus does not affect the dynamics of inflation. It is not completely clear what is the minimum requirement in order for this approximation to be consistent. A sufficient requirement is nevertheless given by $r_* \ll 1$.

Finally the smooth cut in the lower left corner of the parameter space is given by the isocurvature limit, i.e., a lower limit on the magnitude of the effective decay constant Γ. This limit is demonstrated by the line d.

7.3   Scan of the Parameter Space

A thorough scan of the parameter space was performed in articles **I** and **II**. We considered values of n from 0 to 6 and values of m from 10^6GeV to 10^{10}GeV. We then scanned through the parameter space of (H_*, r_*) for all combinations of m and n.

The numerical results confirm the qualitative understanding of the oscillations presented in chapter 6. From the plots in article **I** we see that for $n = 6$ there are no oscillations in the non-quadratic regime of the potential, and thus there are no oscillations either in the parameter space. Also for $n = 0$ the oscillations are so rapid in the non-quadratic part, that the phase thereof does not freeze in but rather is wiped out by the transition from the non-quadratic regime to the quadratic regime. Here the transition lasts several oscillation cycles.

For $n = 2$ and $n = 4$ the oscillations in the non-quadratic potential result in large oscillations in the parameter space. The values of Γ, r_{dec}, f_{NL} and g_{NL} all oscillate, or are strongly dependent on small alterations of the initial conditions. These oscillations result in such regions in the parameter space being allowed, which would seem to be disallowed by naïve analysis. Specifically, since both f_{NL} and g_{NL} oscillate, even in areas where the analytical approximations would give large values for f_{NL} and g_{NL}, there are always points where at least the other one is zero. The observational limits for g_{NL} are much less stringent than for f_{NL}, and thus points around $f_{\text{NL}} \sim 0$ are usually allowed.

In general the results of article **II** indicate that there is not much parameter space left for the $n = 0$ case.[1] Instead, for $n = 2$, 4 and 6 there are large areas in the parameter space which are compatible with observations. Since f_{NL} and g_{NL} oscillate wildly, their absolute magnitude is nevertheless large in most of the allowed regions. Large non-Gaussianity here of course means allowed by observations but significantly non-zero, and perhaps detectable with next generation CMB experiments, such as Planck.

The values of the decay constant Γ mostly populate the lower limit imposed by the isocurvature bound. *A priori* this of course is not a nuissance, however, one can argue that the model implies fine tuning if the curvaton is required to decay just before DM decoupling. The small values of Γ can also be a problem for a model builder, since this suggests very small coupling costants.

7.4   The TeV-mass Curvaton

There are strong theoretical hints that there may be significant new physics on the TeV scale. Furthermore current and future experiments, such as the LHC, might discover new degrees of freedom which might function as a curvaton field [102]. Thus in article **III** we took the parameter choice $m = 1$ TeV as a specific example.

As demonstrated in section 5, for a curvaton with a TeV mass, the assumption of a quadratic potential is not self-consistent, since even the weak self-interactions of equation (5.9) will always play a significant role in the evolution of the curvaton. Furthermore, we found that even though *a priori* unconstrained, n can take only the

---

[1] Note that since we chose the potential to have the form of equation (5.9), the $n = 0$ corresponds to a very strong coupling. If one would add a small coupling constant, then this would leave more parameter space allowed.

value $n = 4$. This is due to the fact that for other choices of n the curvaton needs to decay so late that the isocurvature limit rules these scenarios out, and only the $n = 4$ potential offers sufficient amplification of the perturbations due to the non-linearities so that all constraints are satisified. The part of the parameter space which is allowed for $n = 4$ is then limited to isolated stripes in the (H_*, r_*)-space. Their total area is small compared to the total parameter range, but still sufficiently large.

The TeV mass curvaton requires values for Γ that are very close to the lower limit imposed by the isocurvature bound. Though this is not a problem for the curvaton model in general, it is a problem for most realistic particle physics motivated models. One of the most attractive candidates of scalar fields to function as the curvaton are the flat directions present in supersymmetric theories. Specifically, the widely studied Minimally Supersymmetric Standard Model, or MSSM, which is one of the most popular candidates for extensions of the Standard Model, feature a large number of these flat directions (for a review, see e.g. [103] and references therein). These flat directions have usually self-interactions of the form of equation (5.9), and thus are viable candidates for a curvaton scenario. Indeed, MSSM flat directions have been suggested to work as a curvaton previously [104–109]. Nevertheless, the values of decay constant found in article **III** are very small, since the couplings that they apply are smaller than the couplings present in the Standard Model, and thus also in the MSSM.

7.4.1 Additional Mechanisms to Facilitate Small Values of Γ

If the actual couplings are larger than suggested by the numerical values of Γ found in the scan of the parameter space, than additional mechanisms are required to explain why the curvaton decays so late.

One of the possibilites is so called kinematic blocking. Here the idea is that the fields to which the curvaton is supposed to decay acquire an effective mass that is propotional to the coupling constant and the VEV of the curvaton. If the curvaton has a sufficiently large VEV, than it might be that the would-be decay products have such a large mass that the process of the curvaton decay to the other particles might be kinematically blocked. A real field oscillating around its minimum always of course passes through zero, and thus the VEV of the field also goes to zero. Thus kinematic blocking is possible only if the oscillating field is complex. Though the analysis present in this work concerns only real fields, in the article **III** we argue that if a complex field is oscillating around its minimum with sufficiently small angular momentum, the dynamics that it experiences are very similar to those experienced by a real field. Thus the small effective value of Γ might be explained by the decay channels of the curvaton being kinematically blocked. In the cases where the curvaton field oscillates near zero preheating type phenomena will, however, become important [105, 110–112].

Also note, that what matters is not really where the energy density is, e.g. in the curvaton or in the background, but rather the equation of state of the energy compo-

nent. Thus, if the curvaton decays into an energy component which has the equation of state of matter, then this effectively delays its decay. One such possibility is Q-balls [113, 114] which are macroscopic exitations of complex scalar fields. A collection of Q-balls would have the correct equation of state, $w = 0$, and as the Q-balls decay through surface evaporation, the decay into radiation can be delayed [115, 116].

Chapter 8

Conclusions

In this thesis we have studied the ability of curvaton models to produce the primordial perturbations. Specifically we have documented the behaviour and dynamics of self-interacting curvaton models, and discussed the allowed regions in the parameter space of these models.

It seems plausible that the curvaton, like any other scalar field, has some self-interactions. The type of self-interactions that we consider here has the most simplest functional form imaginable, that is, a monomial. Furthermore, we assume that the mass scale suppressing the self-interaction is the Planck scale, i.e., the highest scale where "conventional" physics is thought to apply, and thus the self-interaction is very weak. In this sense our assumption on the form of the self-interaction is very minimal and well motivated.

As discussed in [86–89, 97, 107, 111, 117, 118], even small deviations from the extensively studied quadratic potential [80] can cause significant effects. In fact, even the type of potential that we consider has been studied for example in [107]. Nevertheless, we have presented for the first time thorough analysis of the dynamics of the self-interacting model. The crucial ingredient for this compared to the previous work was the numerical solution of the equations of motion. In fact, the interesting oscillatory features are completely absent when modeling the evolution of the curvaton with approximative scaling laws.

The self-interactions of the model affect the dynamics of the system in much more drastic ways than one would suspect after naïve analysis: The non-linearity introduced by the self-interactions changes drastically the predictions of the self-interacting curvaton models in wide regions in the parameter space. The slow oscillations in the non-quadratic part of the potential cause the phase of those oscillations to be frozen in to the final value of ζ and derivatives of N, and thus cause oscillations in the parameter space.

The oscillatory behaviour caused by the self-interaction produces also typically large values of f_{NL} and/or g_{NL}. This is caused by the oscillatory behaviour of the

derivatives of N. Although the analytical results $1/r_{\text{dec}}$ and $1/r_{\text{dec}}^2$ capture the non-Gaussianity originating from the subdominance of the curvaton during its decay, they fail to describe the non-Gaussianity originating from the oscillations in the non-quadratic part of the potential. Indeed, we have shown that the non-Gaussianity of the latter type is usually the dominant contribution in the self-interacting models.

Even though the possible parameter space of the self-interacting curvaton model is limited by several observational limits, there remains large regions in the parameter space left for which a self-interacting curvaton would produce perturbations compatible with observations, with different combinations of n and m. For a curvaton with a mass of TeV scale we have shown that the only possible Planck suppressed monomial self-interaction has the power σ^8, since all other choices of n fail to produce the observed perturbations.

The self-interacting curvaton scenario has several intersting properties that are quite rare in other inflationary scenarios. Since f_{NL} and g_{NL} oscillate, they can have either sign. In fact, since they oscillate there are regions in the parameter space where f_{NL} is negligible, and the dominant contribution to non-Gaussianity is given by g_{NL}. (See also [87].)

The decay of the curvaton has not been studied in detail here, as we have merely assumed that the decay processes are well described by an effective decay constant. The values of the decay constant are quite small, and imply weak couplings to known physics. Also preheating type phenomena related to the decay might play a significant role and modify the results for e.g. non-Gaussianity significantly [105, 110–112].

A scenario with mixed perturbations from both the curvaton and inflaton or perhaps from multiple curvatons should be studied with these self-interactions in mind. Since the curvaton can produce (extremely) large values of f_{NL} and g_{NL}, one alternative is that where as most of the amplitude of the perturbations might come from an inflaton with nearly Gaussian statistics, a very subdominant curvaton might produce a smaller perturbation component, but with such a large non-Gaussianity that the non-Gaussianity of the final perturbations might be dominated by the perturbations from the curvaton.

Bibliography

[1] K. Enqvist, S. Nurmi, G. Rigopoulos, O. Taanila, and T. Takahashi, *The Subdominant Curvaton*, *JCAP* **0911** (2009) 003, [`arXiv:0906.3126`].

[2] K. Enqvist, S. Nurmi, O. Taanila, and T. Takahashi, *Non-Gaussian Fingerprints of Self-Interacting Curvaton*, *JCAP* **1004** (2010) 009, [`arXiv:0912.4657`].

[3] K. Enqvist, A. Mazumdar, and O. Taanila, *The TeV-mass curvaton*, *JCAP* **1009** (2010) 030, [`arXiv:1007.0657`].

[4] R. A. Alpher, H. Bethe, and G. Gamow, *The origin of chemical elements*, *Phys. Rev.* **73** (1948) 803–804.

[5] B. Fields and S. Sarkar, *Big-bang nucleosynthesis (PDG mini-review)*, `astro-ph/0601514`.

[6] G. Steigman, *Primordial Nucleosynthesis: The Predicted and Observed Abundances and Their Consequences*, `arXiv:1008.4765`.

[7] G. Lemaitre, *The expanding universe*, *Gen. Rel. Grav.* **29** (1997) 641–680.

[8] A. A. Friedmann, *Über die Krümmung des Raumes*, *Z. Phys. A.* **10** (1922) 377–386.

[9] H. P. Robertson, *Kinematics and world-structure*, *Astrophys. J.* **82** (1935) 284.

[10] H. P. Robertson, *Kinematics and world-structure ii*, *Astrophys. J.* **83** (1936) 187.

[11] H. P. Robertson, *Kinematics and world-structure iii*, *Astrophys. J.* **83** (1935) 357.

[12] M. Vardanyan, R. Trotta, and J. Silk, *How flat can you get? A model comparison perspective on the curvature of the Universe*, *Mon. Not. Roy. Astron. Soc.* **397** (2009) 431–444, [`arXiv:0901.3354`].

[13] E. Komatsu *et. al.*, *Seven-Year Wilkinson Microwave Anisotropy Probe (WMAP) Observations: Cosmological Interpretation*, `arXiv:1001.4538`.

[14] E. Hubble, *A relation between distance and radial velocity among extra–galactic nebulae*, *Proc. Nat. Acad. Sci.* **15** (1929) 168–173.

[15] R. H. Dicke, P. J. E. Peebles, P. G. Roll, and D. T. Wilkinson, *Cosmic Black-Body Radiation*, *Astrophys. J.* **142** (1965) 414–419.

[16] A. A. Penzias and R. W. Wilson, *A Measurement of excess antenna temperature at 4080- Mc/s*, *Astrophys. J.* **142** (1965) 419–421.

[17] C. L. Bennett *et. al.*, *4-Year COBE DMR Cosmic Microwave Background Observations: Maps and Basic Results*, *Astrophys. J.* **464** (1996) L1–L4, [`astro-ph/9601067`].

[18] D. Baumann, *TASI Lectures on Inflation*, `arXiv:0907.5424`.

[19] A. H. Guth, *The Inflationary Universe: A Possible Solution to the Horizon and Flatness Problems*, *Phys. Rev.* **D23** (1981) 347–356.

[20] A. A. Starobinsky, *Spectrum of relict gravitational radiation and the early state of the universe*, *JETP Lett.* **30** (1979) 682–685.

[21] A. A. Starobinsky, *A new type of isotropic cosmological models without singularity*, *Phys. Lett.* **B91** (1980) 99–102.

[22] A. R. Liddle, P. Parsons, and J. D. Barrow, *Formalizing the slow roll approximation in inflation*, *Phys. Rev.* **D50** (1994) 7222–7232, [`astro-ph/9408015`].

[23] P. J. Steinhardt and M. S. Turner, *A Prescription for Successful New Inflation*, *Phys. Rev.* **D29** (1984) 2162–2171.

[24] D. S. Salopek and J. R. Bond, *Nonlinear evolution of long wavelength metric fluctuations in inflationary models*, *Phys. Rev.* **D42** (1990) 3936–3962.

[25] A. R. Liddle and D. H. Lyth, *COBE, gravitational waves, inflation and extended inflation*, *Phys. Lett.* **B291** (1992) 391–398, [`astro-ph/9208007`].

[26] D. H. Lyth and A. Riotto, *Particle physics models of inflation and the cosmological density perturbation*, *Phys. Rept.* **314** (1999) 1–146, [`hep-ph/9807278`].

[27] A. Vilenkin and L. H. Ford, *Gravitational Effects upon Cosmological Phase Transitions*, *Phys. Rev.* **D26** (1982) 1231.

[28] A. D. Linde, *Scalar Field Fluctuations in Expanding Universe and the New Inflationary Universe Scenario*, *Phys. Lett.* **B116** (1982) 335.

[29] A. A. Starobinsky, *Dynamics of Phase Transition in the New Inflationary Universe Scenario and Generation of Perturbations*, *Phys. Lett.* **B117** (1982) 175–178.

[30] T. S. Bunch and P. C. W. Davies, *Quantum Field Theory in de Sitter Space: Renormalization by Point Splitting*, *Proc. Roy. Soc. Lond.* **A360** (1978) 117–134.

[31] **WMAP** Collaboration, E. Komatsu *et. al.*, *Five-Year Wilkinson Microwave Anisotropy Probe Observations: Cosmological Interpretation*, *Astrophys. J. Suppl.* **180** (2009) 330–376, [arXiv:0803.0547].

[32] **WMAP** Collaboration, J. Dunkley *et. al.*, *Five-Year Wilkinson Microwave Anisotropy Probe (WMAP) Observations: Likelihoods and Parameters from the WMAP data*, *Astrophys. J. Suppl.* **180** (2009) 306–329, [arXiv:0803.0586].

[33] **SDSS** Collaboration, M. Tegmark *et. al.*, *Cosmological Constraints from the SDSS Luminous Red Galaxies*, *Phys. Rev.* **D74** (2006) 123507, [astro-ph/0608632].

[34] **The 2dFGRS** Collaboration, S. Cole *et. al.*, *The 2dF Galaxy Redshift Survey: Power-spectrum analysis of the final dataset and cosmological implications*, *Mon. Not. Roy. Astron. Soc.* **362** (2005) 505–534, [astro-ph/0501174].

[35] S. Dodelson, *Modern cosmology*. Amsterdam, Netherlands: Academic Pr. (2003) 440 p.

[36] L. Sriramkumar, *An introduction to inflation and cosmological perturbation theory*, arXiv:0904.4584.

[37] S. Matarrese, S. Mollerach, and M. Bruni, *Second-order perturbations of the Einstein-de Sitter universe*, *Phys. Rev.* **D58** (1998) 043504, [astro-ph/9707278].

[38] H. Kurki-Suonio, "Cosmological Perturbation Theory." 2007.

[39] J. M. Bardeen, P. J. Steinhardt, and M. S. Turner, *Spontaneous Creation of Almost Scale - Free Density Perturbations in an Inflationary Universe*, *Phys. Rev.* **D28** (1983) 679.

[40] M. Sasaki, *Large Scale Quantum Fluctuations in the Inflationary Universe*, *Prog. Theor. Phys.* **76** (1986) 1036.

[41] V. F. Mukhanov, *Quantum Theory of Gauge Invariant Cosmological Perturbations*, *Sov. Phys. JETP* **67** (1988) 1297–1302.

[42] D. Wands, K. A. Malik, D. H. Lyth, and A. R. Liddle, *A new approach to the evolution of cosmological perturbations on large scales*, *Phys. Rev.* **D62** (2000) 043527, [`astro-ph/0003278`].

[43] J. Garcia-Bellido and D. Wands, *Metric perturbations in two-field inflation*, *Phys. Rev.* **D53** (1996) 5437–5445, [`astro-ph/9511029`].

[44] K. A. Malik and D. Wands, *Gauge-invariant variables on cosmological hypersurfaces*, `gr-qc/9804046`.

[45] A. J. Christopherson and K. A. Malik, *The non-adiabatic pressure in general scalar field systems*, *Phys. Lett.* **B675** (2009) 159–163, [`arXiv:0809.3518`].

[46] A. A. Starobinsky, *Multicomponent de Sitter (Inflationary) Stages and the Generation of Perturbations*, *JETP Lett.* **42** (1985) 152–155.

[47] M. Sasaki and E. D. Stewart, *A General analytic formula for the spectral index of the density perturbations produced during inflation*, *Prog. Theor. Phys.* **95** (1996) 71–78, [`astro-ph/9507001`].

[48] M. Sasaki and T. Tanaka, *Super-horizon scale dynamics of multi-scalar inflation*, *Prog. Theor. Phys.* **99** (1998) 763–782, [`gr-qc/9801017`].

[49] D. H. Lyth and D. Wands, *Conserved cosmological perturbations*, *Phys. Rev.* **D68** (2003) 103515, [`astro-ph/0306498`].

[50] D. H. Lyth, K. A. Malik, and M. Sasaki, *A general proof of the conservation of the curvature perturbation*, *JCAP* **0505** (2005) 004, [`astro-ph/0411220`].

[51] G. I. Rigopoulos and E. P. S. Shellard, *The Separate Universe Approach and the Evolution of Nonlinear Superhorizon Cosmological Perturbations*, *Phys. Rev.* **D68** (2003) 123518, [`astro-ph/0306620`].

[52] M. Abramowitz and I. Stegun, eds., *Handbook of Mathematical Functions*. Dover Publications, 1972.

[53] M. S. Turner, *Coherent Scalar Field Oscillations in an Expanding Universe*, *Phys. Rev.* **D28** (1983) 1243.

[54] K. Enqvist and M. S. Sloth, *Adiabatic CMB perturbations in pre big bang string cosmology*, *Nucl. Phys.* **B626** (2002) 395–409, [`hep-ph/0109214`].

[55] D. H. Lyth and D. Wands, *Generating the curvature perturbation without an inflaton*, *Phys. Lett.* **B524** (2002) 5–14, [`hep-ph/0110002`].

[56] T. Moroi and T. Takahashi, *Effects of cosmological moduli fields on cosmic microwave background*, *Phys. Lett.* **B522** (2001) 215–221, [`hep-ph/0110096`].

[57] A. D. Linde and V. F. Mukhanov, *Nongaussian isocurvature perturbations from inflation*, *Phys. Rev.* **D56** (1997) 535–539, [astro-ph/9610219].

[58] S. Mollerach, *Isocurvature baryon perturbations and inflation*, *Phys. Rev.* **D42** (1990) 313–325.

[59] D. Langlois and F. Vernizzi, *Mixed inflaton and curvaton perturbations*, *Phys. Rev.* **D70** (2004) 063522, [astro-ph/0403258].

[60] G. Lazarides, R. R. de Austri, and R. Trotta, *Constraints on a mixed inflaton and curvaton scenario for the generation of the curvature perturbation*, *Phys. Rev.* **D70** (2004) 123527, [hep-ph/0409335].

[61] F. Ferrer, S. Rasanen, and J. Valiviita, *Correlated isocurvature perturbations from mixed inflaton- curvaton decay*, *JCAP* **0410** (2004) 010, [astro-ph/0407300].

[62] T. Moroi, T. Takahashi, and Y. Toyoda, *Relaxing constraints on inflation models with curvaton*, *Phys. Rev.* **D72** (2005) 023502, [hep-ph/0501007].

[63] K. Ichikawa, T. Suyama, T. Takahashi, and M. Yamaguchi, *Non-Gaussianity, Spectral Index and Tensor Modes in Mixed Inflaton and Curvaton Models*, *Phys. Rev.* **D78** (2008) 023513, [arXiv:0802.4138].

[64] D. Langlois, F. Vernizzi, and D. Wands, *Non-linear isocurvature perturbations and non- Gaussianities*, *JCAP* **0812** (2008) 004, [arXiv:0809.4646].

[65] H. Assadullahi, J. Valiviita, and D. Wands, *Primordial non-Gaussianity from two curvaton decays*, *Phys. Rev.* **D76** (2007) 103003, [arXiv:0708.0223].

[66] J. Valiviita, H. Assadullahi, and D. Wands, *Primordial non-gaussianity from multiple curvaton decay*, arXiv:0806.0623.

[67] K. A. Malik, D. Wands, and C. Ungarelli, *Large-scale curvature and entropy perturbations for multiple interacting fluids*, *Phys. Rev.* **D67** (2003) 063516, [astro-ph/0211602].

[68] E. Komatsu and D. N. Spergel, *Acoustic signatures in the primary microwave background bispectrum*, *Phys. Rev.* **D63** (2001) 063002, [astro-ph/0005036].

[69] J. M. Maldacena, *Non-Gaussian features of primordial fluctuations in single field inflationary models*, *JHEP* **05** (2003) 013, [astro-ph/0210603].

[70] D. H. Lyth and Y. Rodriguez, *The inflationary prediction for primordial non-gaussianity*, *Phys. Rev. Lett.* **95** (2005) 121302, [astro-ph/0504045].

[71] N. Bartolo, E. Komatsu, S. Matarrese, and A. Riotto, *Non-Gaussianity from inflation: Theory and observations*, *Phys. Rept.* **402** (2004) 103–266, [`astro-ph/0406398`].

[72] D. Wands, *Local non-Gaussianity from inflation*, *Class. Quant. Grav.* **27** (2010) 124002, [`arXiv:1004.0818`].

[73] C. T. Byrnes, S. Nurmi, G. Tasinato, and D. Wands, *Scale dependence of local f_{NL}*, *JCAP* **1002** (2010) 034, [`arXiv:0911.2780`].

[74] C. T. Byrnes, M. Gerstenlauer, S. Nurmi, G. Tasinato, and D. Wands, *Scale-dependent non-Gaussianity probes inflationary physics*, `arXiv:1007.4277`.

[75] C. T. Byrnes, K. Enqvist, and T. Takahashi, *Scale-dependence of Non-Gaussianity in the Curvaton Model*, `arXiv:1007.5148`.

[76] V. Desjacques and U. Seljak, *Signature of primordial non-Gaussianity of phi3-type in the mass function and bias of dark matter haloes*, *Phys. Rev.* **D81** (2010) 023006, [`arXiv:0907.2257`].

[77] **Planck** Collaboration, *Planck: The scientific programme*, `astro-ph/0604069`.

[78] A. Slosar, C. Hirata, U. Seljak, S. Ho, and N. Padmanabhan, *Constraints on local primordial non-Gaussianity from large scale structure*, *JCAP* **0808** (2008) 031, [`arXiv:0805.3580`].

[79] P. Creminelli and M. Zaldarriaga, *Single field consistency relation for the 3-point function*, *JCAP* **0410** (2004) 006, [`astro-ph/0407059`].

[80] D. H. Lyth, C. Ungarelli, and D. Wands, *The primordial density perturbation in the curvaton scenario*, *Phys. Rev.* **D67** (2003) 023503, [`astro-ph/0208055`].

[81] N. Bartolo, S. Matarrese, and A. Riotto, *On non-Gaussianity in the curvaton scenario*, *Phys. Rev.* **D69** (2004) 043503, [`hep-ph/0309033`].

[82] C. Gordon and K. A. Malik, *WMAP, neutrino degeneracy and non-Gaussianity constraints on isocurvature perturbations in the curvaton model of inflation*, *Phys. Rev.* **D69** (2004) 063508, [`astro-ph/0311102`].

[83] K. A. Malik and D. H. Lyth, *A numerical study of non-gaussianity in the curvaton scenario*, *JCAP* **0609** (2006) 008, [`astro-ph/0604387`].

[84] M. Sasaki, J. Valiviita, and D. Wands, *Non-gaussianity of the primordial perturbation in the curvaton model*, *Phys. Rev.* **D74** (2006) 103003, [`astro-ph/0607627`].

[85] J. Valiviita, M. Sasaki, and D. Wands, *Non-Gaussianity and constraints for the variance of perturbations in the curvaton model*, `astro-ph/0610001`.

[86] K. Enqvist and S. Nurmi, *Non-gaussianity in curvaton models with nearly quadratic potential*, *JCAP* **0510** (2005) 013, [`astro-ph/0508573`].

[87] K. Enqvist and T. Takahashi, *Signatures of Non-Gaussianity in the Curvaton Model*, *JCAP* **0809** (2008) 012, [`arXiv:0807.3069`].

[88] Q.-G. Huang, *Curvaton with Polynomial Potential*, *JCAP* **0811** (2008) 005, [`arXiv:0808.1793`].

[89] P. Chingangbam and Q.-G. Huang, *The Curvature Perturbation in the Axion-type Curvaton Model*, *JCAP* **0904** (2009) 031, [`arXiv:0902.2619`].

[90] R. Bean, J. Dunkley, and E. Pierpaoli, *Constraining Isocurvature Initial Conditions with WMAP 3- year data*, *Phys. Rev.* **D74** (2006) 063503, [`astro-ph/0606685`].

[91] M. Kawasaki and T. Sekiguchi, *Cosmological Constraints on Isocurvature and Tensor Perturbations*, *Prog. Theor. Phys.* **120** (2008) 995–1016, [`arXiv:0705.2853`].

[92] L. Bergstrom, *Dark Matter Candidates*, *New J. Phys.* **11** (2009) 105006, [`arXiv:0903.4849`].

[93] G. Steigman and M. S. Turner, *Cosmological Constraints on the Properties of Weakly Interacting Massive Particles*, *Nucl. Phys.* **B253** (1985) 375.

[94] M. Srednicki, R. Watkins, and K. A. Olive, *Calculations of relic densities in the early universe*, *Nucl. Phys.* **B310** (1988) 693.

[95] P. Gondolo and G. Gelmini, *Cosmic abundances of stable particles: Improved analysis*, *Nucl. Phys.* **B360** (1991) 145–179.

[96] L. D. Duffy and K. van Bibber, *Axions as Dark Matter Particles*, *New J. Phys.* **11** (2009) 105008, [`arXiv:0904.3346`].

[97] P. Chingangbam and Q.-G. Huang, *New features in curvaton model*, `arXiv:1006.4006`.

[98] K. Dimopoulos, *Can a vector field be responsible for the curvature perturbation in the universe?*, *Phys. Rev.* **D74** (2006) 083502, [`hep-ph/0607229`].

[99] M. Karciauskas, K. Dimopoulos, and D. H. Lyth, *Anisotropic non-Gaussianity from vector field perturbations*, *Phys. Rev.* **D80** (2009) 023509, [`arXiv:0812.0264`].

[100] K. Dimopoulos, M. Karciauskas, and J. M. Wagstaff, *Vector Curvaton without Instabilities*, *Phys. Lett.* **B683** (2010) 298–301, [arXiv:0909.0475].

[101] D. Wands, N. Bartolo, S. Matarrese, and A. Riotto, *An observational test of two-field inflation*, *Phys. Rev.* **D66** (2002) 043520, [astro-ph/0205253].

[102] G. Kane, (ed.) and A. Pierce, (ed.), *Perspectives on LHC physics*, . Hackensack, USA: World Scientific (2008) 337 p.

[103] K. Enqvist and A. Mazumdar, *Cosmological consequences of MSSM flat directions*, *Phys. Rept.* **380** (2003) 99–234, [hep-ph/0209244].

[104] S. Kasuya, M. Kawasaki, and F. Takahashi, *MSSM curvaton in the gauge-mediated SUSY breaking*, *Phys. Lett.* **B578** (2004) 259–268, [hep-ph/0305134].

[105] R. Allahverdi, K. Enqvist, J. Garcia-Bellido, A. Jokinen, and A. Mazumdar, *MSSM flat direction inflation: slow roll, stability, fine tunning and reheating*, *JCAP* **0706** (2007) 019, [hep-ph/0610134].

[106] R. Allahverdi, K. Enqvist, A. Jokinen, and A. Mazumdar, *Identifying the curvaton within MSSM*, *JCAP* **0610** (2006) 007, [hep-ph/0603255].

[107] K. Enqvist, A. Jokinen, S. Kasuya, and A. Mazumdar, *MSSM flat direction as a curvaton*, *Phys. Rev.* **D68** (2003) 103507, [hep-ph/0303165].

[108] J. McDonald, *Supersymmetric curvatons and phase-induced curvaton fluctuations*, *Phys. Rev.* **D69** (2004) 103511, [hep-ph/0310126].

[109] J. McDonald, *Right-handed sneutrinos as curvatons*, *Phys. Rev.* **D68** (2003) 043505, [hep-ph/0302222].

[110] G. N. Felder, L. Kofman, and A. D. Linde, *Instant preheating*, *Phys. Rev.* **D59** (1999) 123523, [hep-ph/9812289].

[111] K. Enqvist, S. Nurmi, and G. I. Rigopoulos, *Parametric Decay of the Curvaton*, *JCAP* **0810** (2008) 013, [arXiv:0807.0382].

[112] A. Chambers, S. Nurmi, and A. Rajantie, *Non-Gaussianity from resonant curvaton decay*, *JCAP* **1001** (2010) 012, [arXiv:0909.4535].

[113] S. R. Coleman, *Q Balls*, *Nucl. Phys.* **B262** (1985) 263.

[114] A. Kusenko and M. E. Shaposhnikov, *Supersymmetric Q-balls as dark matter*, *Phys. Lett.* **B418** (1998) 46–54, [hep-ph/9709492].

[115] K. Enqvist, S. Kasuya, and A. Mazumdar, *Inflatonic solitons in running mass inflation*, *Phys. Rev.* **D66** (2002) 043505, [hep-ph/0206272].

[116] K. Enqvist, S. Kasuya, and A. Mazumdar, *Adiabatic density perturbations and matter generation from the MSSM*, *Phys. Rev. Lett.* **90** (2003) 091302, [`hep-ph/0211147`].

[117] K. Dimopoulos, G. Lazarides, D. Lyth, and R. Ruiz de Austri, *Curvaton dynamics*, *Phys. Rev.* **D68** (2003) 123515, [`hep-ph/0308015`].

[118] M. Kawasaki, K. Nakayama, and F. Takahashi, *Hilltop Non-Gaussianity*, *JCAP* **0901** (2009) 026, [`arXiv:0810.1585`].